

AD-A086 666

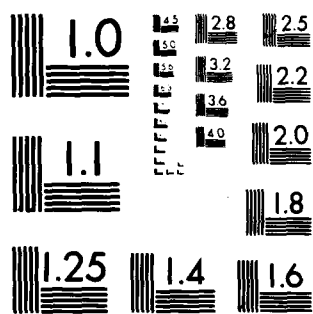
NAVAL ACADEMY ANNAPOLIS MD DIV OF ENGINEERING AND WEAPONS F/G 13/10
A SEARCH FOR THE BEST METHOD TO RIG A RACING SHELL. (U)
MAY 80 C E EVERETT
USNA/EW-9-80

UNCLASSIFIED

NL

1 GA
AC

END
DATE
FILMED
8-80
DTIC

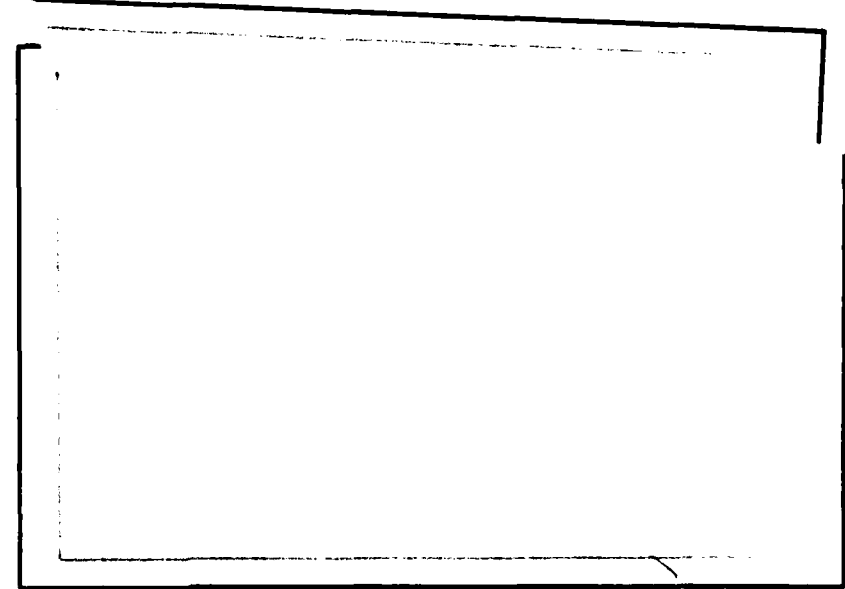


MICROCOPY RESOLUTION TEST CHART
NATIONAL BUREAU OF STANDARDS-1963-A

56
ADA 086666

LEVEL 4

20



UNITED STATES NAVAL ACADEMY
DIVISION OF
ENGINEERING AND WEAPONS
ANNAPOLIS, MARYLAND

DTIC
ELECTE
S JUL 3 1980
A

DISTRIBUTION STATEMENT A
Approved for public release;
Distribution Unlimited

DDC FILE COPY

80 6 16 012

DEPARTMENT OF THE NAVY
United States Naval Academy
Annapolis, Maryland 21402

Division of Engineering and Weapons

14. USNA
Report No. EW-9-80
6. A SEARCH FOR THE BEST METHOD
TO RIG A RACING SHELL.
10. Charles E. Everett, Jr.*
11. 14 May 1980

1263

Approved for public release
Distribution unlimited

*Charles E. Everett, Jr.
Midshipman First Class

DTIC
ELECTE
13 1300

406923

mt

ABSTRACT

A SEARCH FOR THE BEST METHOD TO RIG A RACING SHELL

✓ In today's crew competition one may find different rigging configurations used by the various crew teams. There must be some logical reasoning behind one team using one type of rigging over another one. For the most part, coaches tend to go with personal preferences. This research is designed to find some physical facts as to whether one type of rigging is better for a shell than another. Three different riggings were tested: (1) conventional, port-starboard, (2) tandem at 7 and 6 seats, and (3) tandem at 4 and 5 seats. The shell was equipped with accelerometers which recorded the transverse accelerations. From the data collected plots were made to illustrate the deflections that occurred with each rigging configuration. The results proved that the tandem riggings are more favorable in producing a straighter course for the shell to travel. Since, to my knowledge, this is the first time any test of this type has been conducted, the initial theory that the moments imparted at the riggers affect the overall course of the shell is proved valid. ↙

TABLE OF CONTENTS

	<u>Page</u>
Abstract	iii
INTRODUCTION	1
STATIC ANALYSIS	5
DYNAMIC ANALYSIS	11
EXPERIMENT	16
RESULTS	19
CALCULATIONS	23
DISCUSSION OF RESULTS	38
FUTURE WORK	40
ACKNOWLEDGEMENTS	4
REFERENCES	42
Appendix A Equipment Set-up Sketch.....	A-1 - A-2
Appendix B Computer Program and Required Data.....	B-1 - B-2
Appendix C Natural Vibration Modes Computer Output..	C-1 - C-2
Appendix D Test Data.....	D-1
Appendix E Computer Printout.....	E-1 - E-6

Page E-3 is not missing but is mis-
numbered

Accession For	
NTES GPM&I	<input checked="" type="checkbox"/>
DDC TAB	<input type="checkbox"/>
Unannounced	<input type="checkbox"/>
Justification	
By _____	
Distribution/	
Availability Codes	
Dist.	Avail and/or special
A	

MISSING PAGE BLANK - NOT FILLED

INTRODUCTION

"The winning factor in a crew race is not the chariot but the horses" can be quite true. However, when there are two evenly matched crews in terms of equipment and team members of equal caliber, other factors determine the winner. Each time the coxswain has to use his rudder during a race it slows the shell down, which over a 2000 meter course could determine the winner in a close race. This led to the purpose behind this research in the rigging of crew shells. Is it possible that different rigging configurations of shells have an effect on the course in which the shells will naturally travel, due to the different moments imparted on the shell by the placement of the oars ? The theory used indicates that while the force balance is preserved, the moment balance is not. If there is a difference, it will be in the transverse plane of motion.

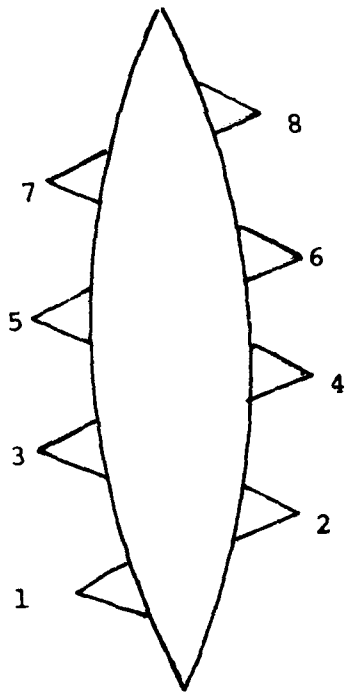
Coaches have as many different ideas about how to rig a shell as there are coaches. Two of the most dominant ideas are the one of "gut feelings" and the other dealing with a numbering game. To some extent, boating a crew has a lot to do with the personality of

the oarsmen and their individual styles and quirks. Therefore, after a coach has determined his best eight oarsmen, he may find that a tandem-rigged shell may best suit his crew vice the conventional, port-starboard rigging. On the other hand, a coach may use the tandem rigging to give one side better leverage so as to overcome any lack of strength that one side shows.

One way to illustrate this idea of different rigging presenting superior leverage over another is to assign values to each rigger. This is done by numbering from the bow down to the stroke, where the bow seat is assigned the number 8 and the stroke seat the number 1; and summing up the numbers on both the port and the starboard sides. The bow rigger received the highest value since by location it has the greatest effect on moving the bow of the shell, hence causing the most rudder to be used to compensate and travel in a straight line. After adding up the numbers, the tandem riggings present a more even comparison whereby having seats 4 and 5 tandem, both sides have equivalent totals. Thus, by using a tandem rigging at 4 and 5, any side forces

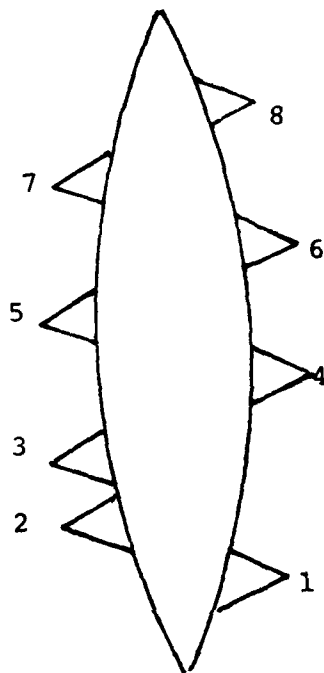
that may occur by using the other rigs should be eliminated. Thereby, according to this evaluation the coxswain need not use the rudder to correct the shell's course as much in order to travel in a straight line.

Conventional



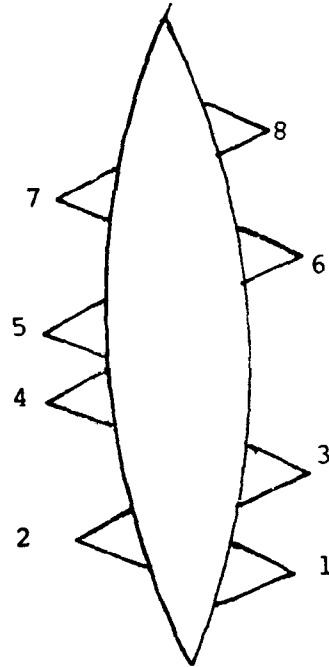
16

Tandem 7 and 6



20 17

Tandem 4 and 5



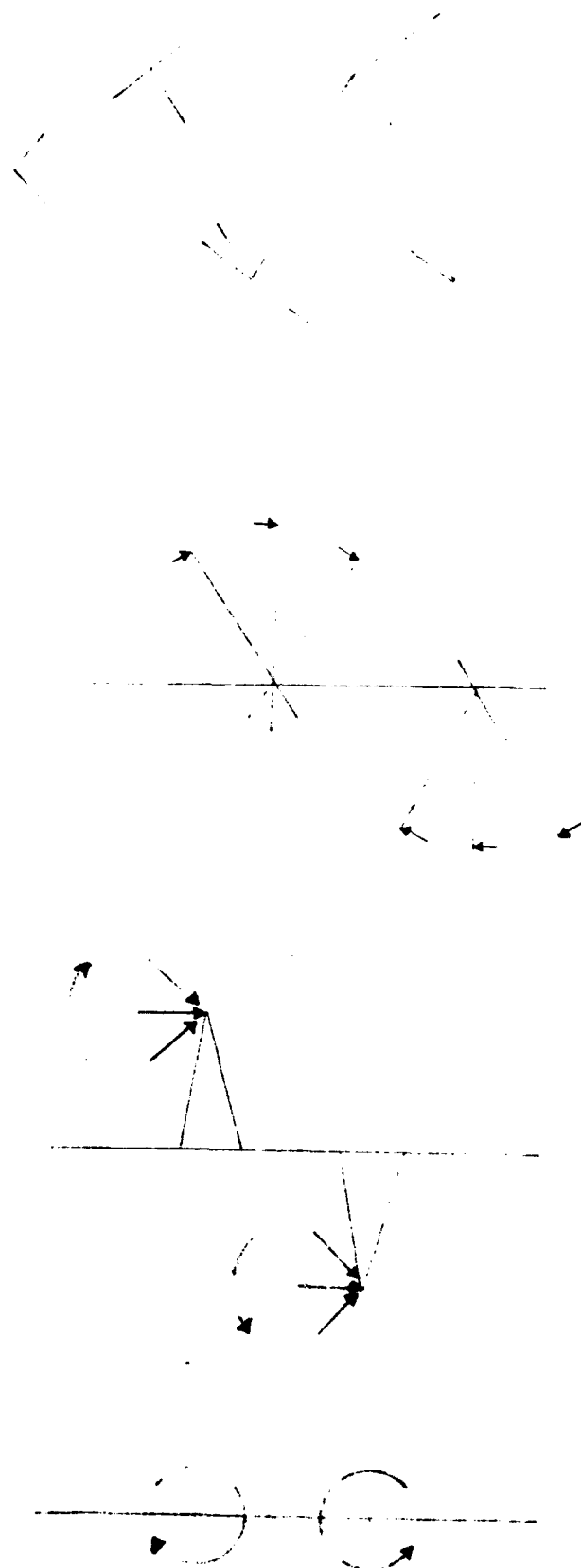
19 18

18

STATIC ANALYSIS

Before the actual experiments were performed on the shell, some theoretical calculations were made. The first step in these calculations was to determine the resultant quasi-static moments imparted to the shell by each oar and the resultant deflection. Figure 1 illustrates how this was accomplished for both a port and starboard oar. Once the moments are aligned in the configuration of the shell's rigging, instantaneous peak loads were applied at each oar location along the shell, treated here as a free-free beam. All load values were assumed to be of equal value. From the load (moment) diagram, one can integrate it to get the slope diagram and with a second integration, the deflection diagram can be obtained. Figures 2, 3, and 4 illustrate this for each of the three rigging configurations being considered. After reviewing each of the three deflection diagrams from this point of view, the rigging using a tandem at seats 7 and 6 seems to be the best. The overall deflection of the shell resembles a sine curve, thus yielding near equal forces on each side of the shell. Tandem rigging at

seats 4 and 5 seems to point out that it is most useful should one side of the crew be physically stronger than the other side. The conventional rigging shows an increasing deflection arm as one moves toward the bow.



Resultant Moments

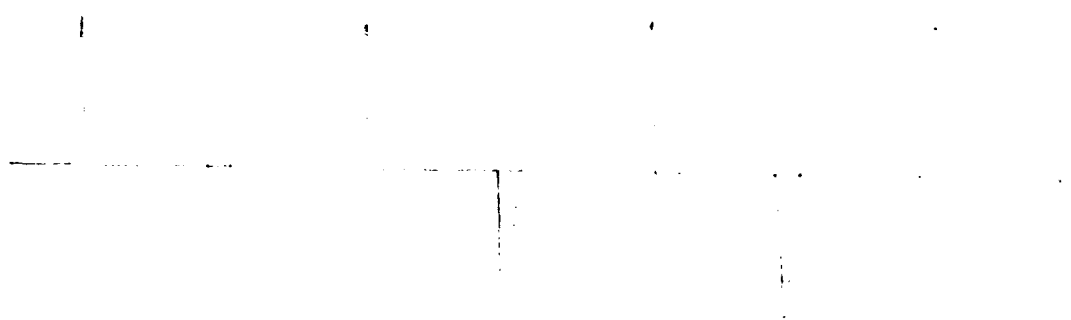
Figure 1

Conventional Rig

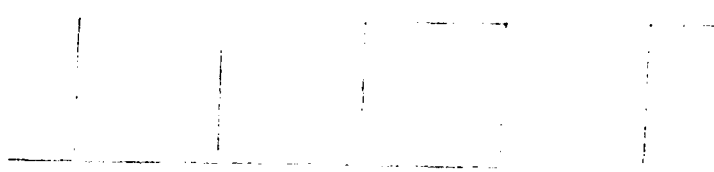
Moments Imparted at Riggers



Instant Peak Moments



Slope Diagram



Deflection Diagram

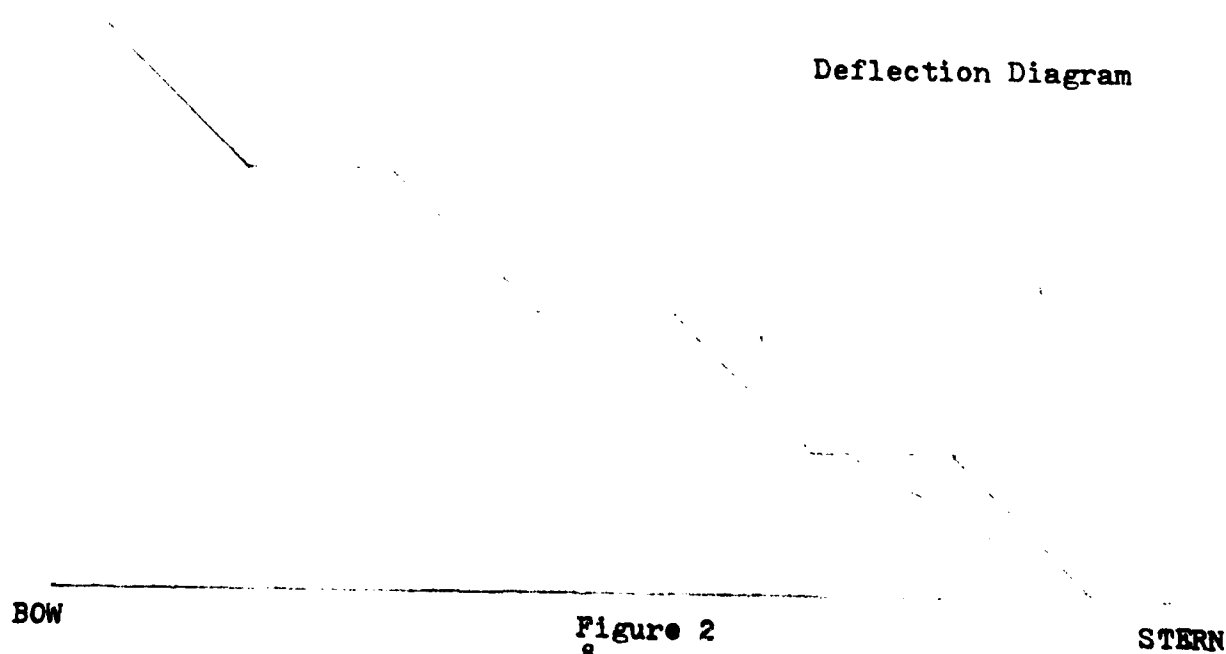


Figure 2
8

Tandem 7&6

Moments Imparted at Riggers

Instant Peak Moments

Slope Diagram

Deflection Diagram

BOW

STERN

Figure 3

Tandem 4&5

Moments Imparted at Riggers

Instant Peak Moments

Slope Diagram

Deflection Diagram

BOW

STERN

Figure 4

DYNAMIC ANALYSIS

As a preliminary search for the vibration that a crew shell may encounter, a computer program, EN***: NATVIBR was used. This program illustrates mode shapes and their relative magnitudes along the length of the shell. Before using this program, body plans of the shell had to be made. The shell was divided into ten stations from which cross-sectional views were drawn, Figure 4a. A mechanical integrator was used to compute the 2nd moment of the structural area for each station. The stations were drawn to scale by offsets obtained from measuring the shell. To ensure accurate readings, each station was traced a minimum of three times by the integrator to obtain an average reading. The inside braces were added in the computations since they added to the longitudinal stiffness. After obtaining the average readings for area, moment of area and moment of inertia, the following equations supplied by the manufacturer were used to calculate the final Area, Moment of Area and Moment of Inertia at each station.

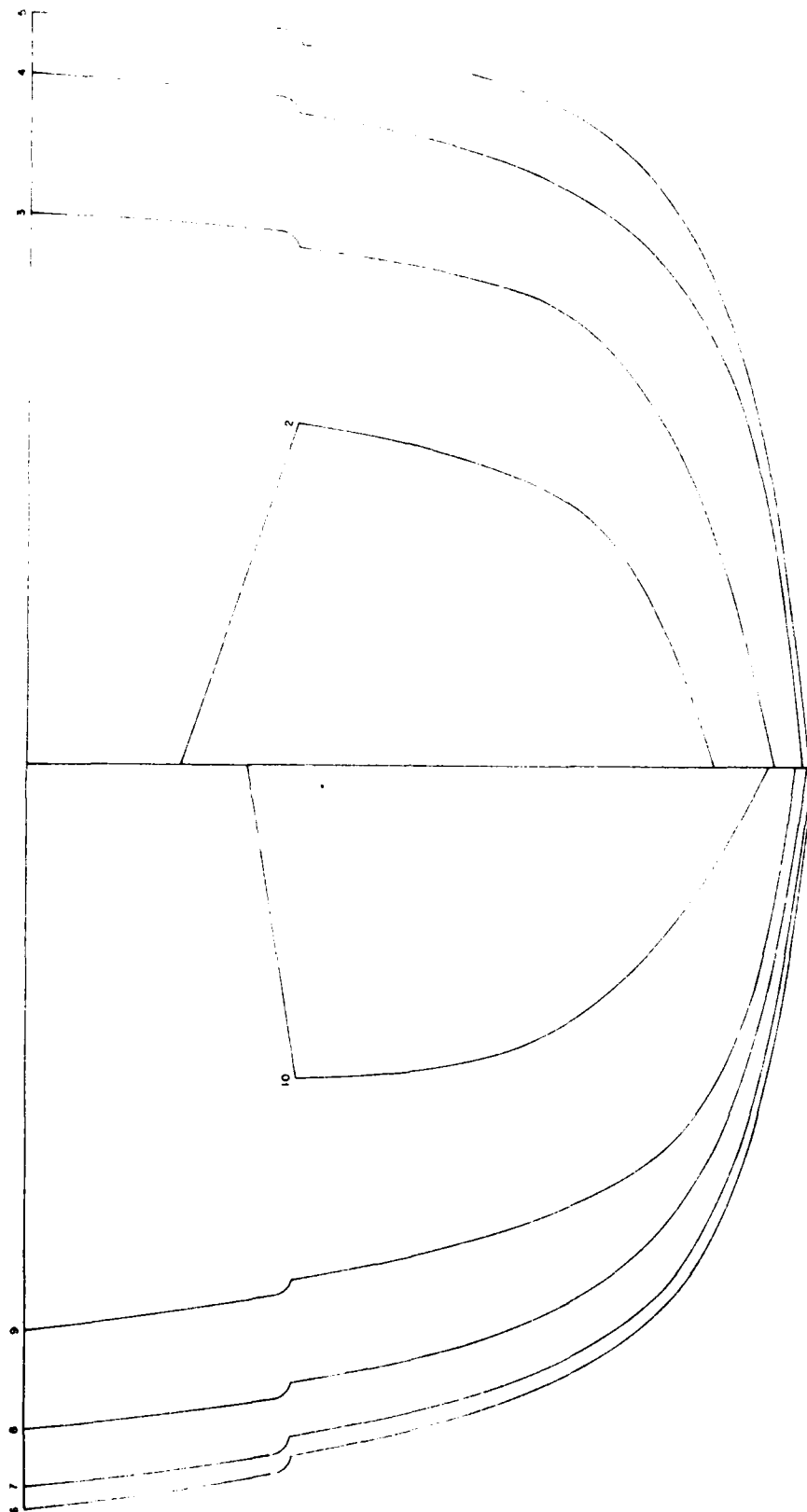
Area	$.04A$	m^2
Moment of Area	$.16m$	m^3
Moment of Inertia	$(.32A - .1I)$	m^4

The input data required to run the computer program for vibration analysis are: Young's Modulus ($E = 13 \times 10^6$ psi for wood), distance between each station, total mass at station per unit length and 2nd Moment of Inertia - obtained from the integration.

When computing the total mass at each station calculations were performed to include the factor of added mass. This was done by following the rules that Dr. L. Landweber and M. C. de Macgro set forth in their paper "Added Mass of Two Dimensional Forms Oscillating in a Free Surface." Two computations were performed: one with and one without the weight of the oars. There was no significant change in the calculated mode shape and natural frequencies when the two were inputted into the computer program. Also required was Z , rotary moment of inertia and KAG, shear deformation value; however, in the case neither value was crucial so an extremely large number was entered for these values.

The output of this program yielded the natural frequencies at different modes. Also, since the results were printed out in a graphical format, the locations

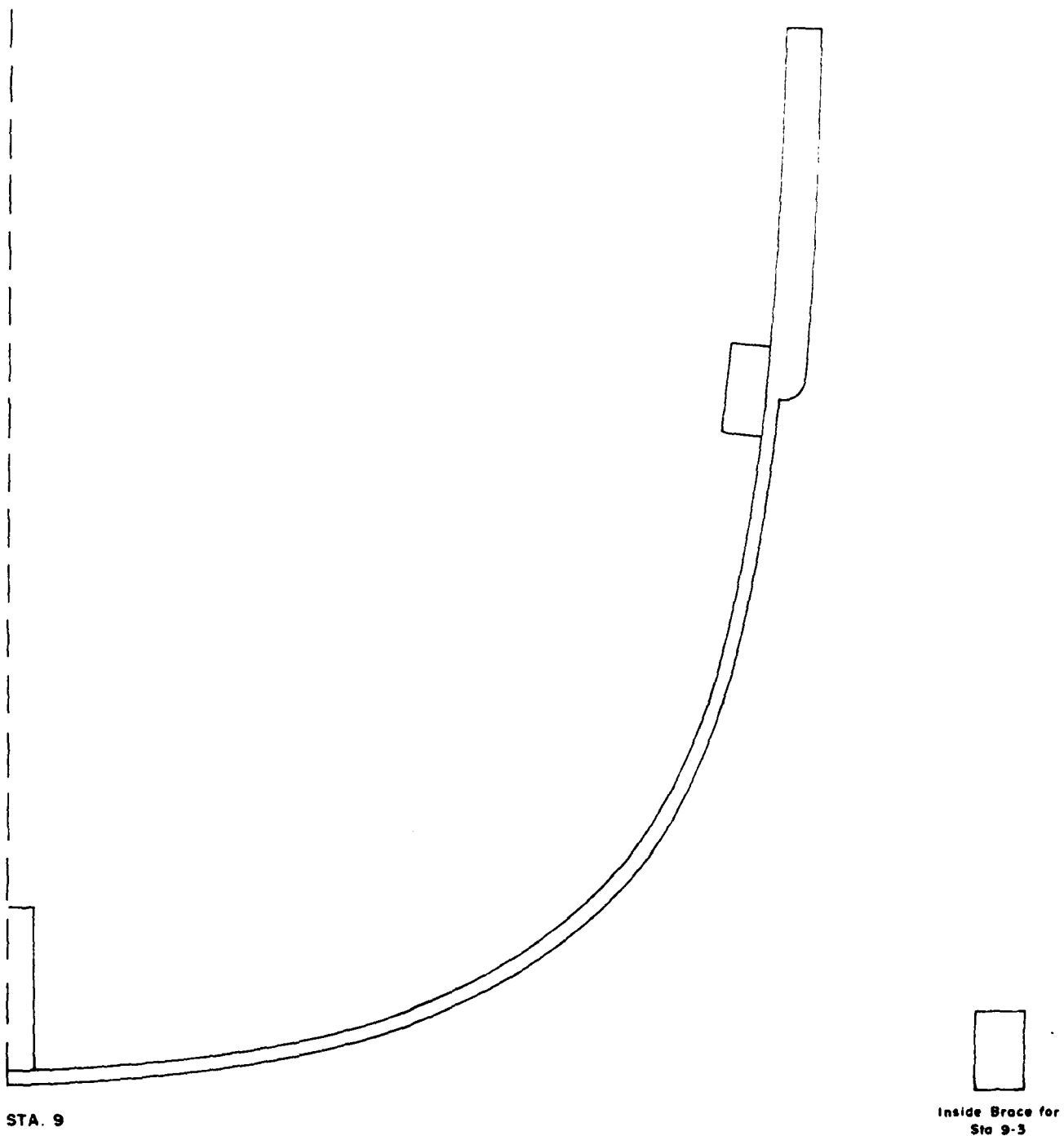
where zero deflection occurs were determined for the shell. This information is later used in the determination of the locations for accelerometers.



Body Plan

Scale $\frac{1}{3}'' = 1''$

Figure 4a 14



Body Plan at Station 9

Scale $1/2" = 1"$

EXPERIMENT

The field experiment used to determine if, in fact, there are measurable variations in the side deflections present due to the different riggings centered around the use of four accelerometers. A George Pocock eight-oared racing shell was used as the test platform.

Four accelerometers were equally separated along the length of the shell and placed on the center line. The reasoning in using four accelerometers is due to the fact that this was the limiting number that the portable data acquisition system can handle. Their location was determined by ABS rules which stated that there should be two placed at the ends and the rest spaced evenly in between. To ensure that the other two accelerometers were not placed on points of predicted nodes, the results of dynamic analysis was used. The node points were computed to be 14.6 ft. and 43.8 ft. from the stern. Ideally, having the accelerometers evenly spaced, they would have been located at 19.5 ft. intervals. However, due to the bracing arrangement, these distances could not be used.

The closest points were used to secure the accelerometers which were located 19 ft. and 39 ft. from the stern. The (1g) accelerometers were all attached together at a common point at the stroke's foot stretcher from which the cable ran over the side to the following chase boat. The chase boat was used to carry the instruments thus avoiding the added weight in the crew shell itself. The equipment used consisted of : (2) 12V batteries, AC-DC converter, accelerometer power supply and a tape recorder. A sketch of the set-up can be found in the appendix A. During the tests, all the data was recorded on an FM modulated frequency tape. After the conclusion of the field test, the tape was taken back to the laboratory and processed through an analog computer; thereby determining the initial responses before going on to a digital computer for a more accurate analysis.

A stroke watch was used to insure that a constant stroke rate was maintained during each period of recording.

The shell was rowed by members of the U. S. Naval Academy Light Weight Crew Team, and the shell averaged 155 pounds per man. The course over which the tests were run was a 500 meter course on College Creek. The general weather conditions were a light rain, no wind and flat water. The shell was rowed with three different rigging configurations: a conventional (alternating port-starboard), tandem at 7 and 6, and tandem at 4 and 5. Two stroke rates were used for each rigging: that of 30 and 32 strokes per minute. At the conclusion of the test runs, the accelerometers were checked to insure proper calibration and zero signal values recorded.

RESULTS

During the course of the data collection, the bow accelerometer's signal became increasingly noisy. Due to this occurrence after the first run, the data from the bow accelerometer was not used. With the loss of the bow accelerometer, the effect on the results were noticable, however not significant. Graphs of the final output were obtainable with three data points and the pattern was consistent. A repeat of the experiment could have insured the proper performance of all four accelerometers; however, due to time constraints, weather conditions and the availability of the crew facilities, the field test could only be performed one time.

For each run of data, a 30-second period was used in the analysis while each run was about 100 seconds in length. From this period a Power Spectrum Density (PSD) was performed. This took the signal and for each frequency from 0 to 30 Hz the maximum PSD was determined. Before filtering the signal, the tape was played and a print out from the

script recorder chart was secured. From this chart of accelerations vs. time, noticable points of the stroke could be identified. At the catch it could be noted when the oar blade was emerged in the water and by speeding up the script chart's speed, any delay inbetween immersion and power application could be ascertained. The release was also quite visible. Upon using filters of 60, 50, 20, 10 and 5 Hz, it was determined that the 50 and 20 Hz filters worked the best to eliminate the higher frequencies while not effecting the overall response sought. The 5 Hz filtered too much and the 60 Hz filtered not enough of the noise for it appeared as if there were some 60 Hz frequency present. The 20 Hz filter was chosen to be used. Figures 5 - 10 show graphically how the max PSD at each accelerometer stands for the different riggings.

Another means to compare the different riggings is to compute the instantaneous deflections that occur at the points along the shell where the accelerometers were located. A listing of the deflections is given in Table 1. The best method to compare the effects of the different rigging configurations on a shell is

in the real time frame, for here can be seen how the shell reacts at a given point in time. Looking at the overall print-out of the different accelerometers, a short time lag can be seen between each accelerometer for a given peak in the read-out indicating that the shell is not rotating as a rigid body. Thus, evidence of a transverse vibration of the shell is shown.

In plotting the conventional rigging on real time, both stroke rates illustrated the same pattern as do the other two configurations. The conventional rig shows a definite pattern of "sway." Figures 11 and 12 support the theory that this rigging produces a sideward pull, thereby causing the coxswain to use his rudder more in order to steer his course. The real time graphs (figures 13 and 14) for the tandem rigging of seats 7 and 6 again follow along the line predicted. The movement illustrated by the accelerometer is similar to that of a sinusoidal. The side forces seen here present opposing forces, hence making for a better overall straight course for the shell to travel. The tandem rigging of seats 4 and 5 did not follow the expectation calculated in the static

analysis. Instead of suggesting an overall pull to one side, the side forces alternated sides in the real time graph. When plotting the PSD data, this rigging seemed to show a fishtail effect. Figures 15 and 16 show this arrangement of side forces.

CALCULATIONS

$$1 \Delta f (\sqrt{\text{PSD}}) = g's$$

$$2 g's \times 32.2 \text{ fps}^2 = \text{fps}^2$$

$$3 \text{ fps}^2 / \omega^2 = \text{deflection in feet}$$

where;

$$\omega = 2\pi f = 2\pi (0.2) = 1.26 \text{ rad/sec}$$

$$\Delta f = 0.2$$

$$0.2 (\sqrt{0.2713 \times 10^{-2}}) = 0.010$$

$$0.010 \times 32.2 \text{ fps}^2 = 0.335 \text{ fps}^2$$

$$0.335 \text{ fps}^2 / (1.26 \text{ rad/sec})^2 = 0.212 \text{ ft}$$

ACCELEROMETER MEASUREMENTS

Tandem 4 & 5

Tandem 7 & 6

Conventional

Stroke Rate	Deflection \bar{X} (ft)	PSD (max)	HZ	Deflection \bar{X} (ft)	PSD (max)	HZ	Deflection \bar{X} (ft)	PSD (max)	HZ
BOW									
30	0.212	0.2713×10^{-2}	0.2						
32									
MID B									
30	0.239	0.3425×10^{-2}	0.2	0.206	0.2568×10^{-2}	0.2	0.088	0.4682×10^{-3}	0.2
32	0.189	0.2093×10^{-2}	0.2	0.182	0.1990×10^{-2}	0.2	0.099	0.5883×10^{-2}	0.2
MID S									
30	0.115	0.7994×10^{-3}	0.2	0.185	0.2060×10^{-2}	0.2	0.193	0.2239×10^{-2}	0.2
32	0.129	0.1005×10^{-2}	0.2	0.204	0.2496×10^{-2}	0.2	0.189	0.2152×10^{-2}	0.2
STERN									
30	0.373	0.8365×10^{-2}	0.2	0.443	0.1180×10^{-1}	0.2	0.391	0.9214×10^{-2}	0.2
32	0.343	0.7075×10^{-2}	0.2	0.472	0.1340×10^{-1}	0.2	0.406	0.9915×10^{-2}	0.2

TABLE 1

REAL TIME

Stroke Rate	Rigging	Bow	Mid B	Mid S	Stern	Time (Sec)
30	Conventional	-0.18*	0.09	0.07	0.17	49
	Tanden 7 & 6	--	0.10	-0.09	-0.03	57.5
	Tandem 4 & 5	--	0.06	-0.08	0.06	48
32	Conventional	--	0.14	0.06	0.26	49.5
	Tanden 7 & 6	--	0.08	-0.06	-0.10	48
	Tandem 4 & 5	---	0.11	-0.03	0.15	45.5

* Reverse (+) Axis

Distances accelerometers from stern

Stern 1 ft
Mid S 19 ft
Mid B 39 ft
Bow 57.5 ft

LOA 58.5'

TABLE 2

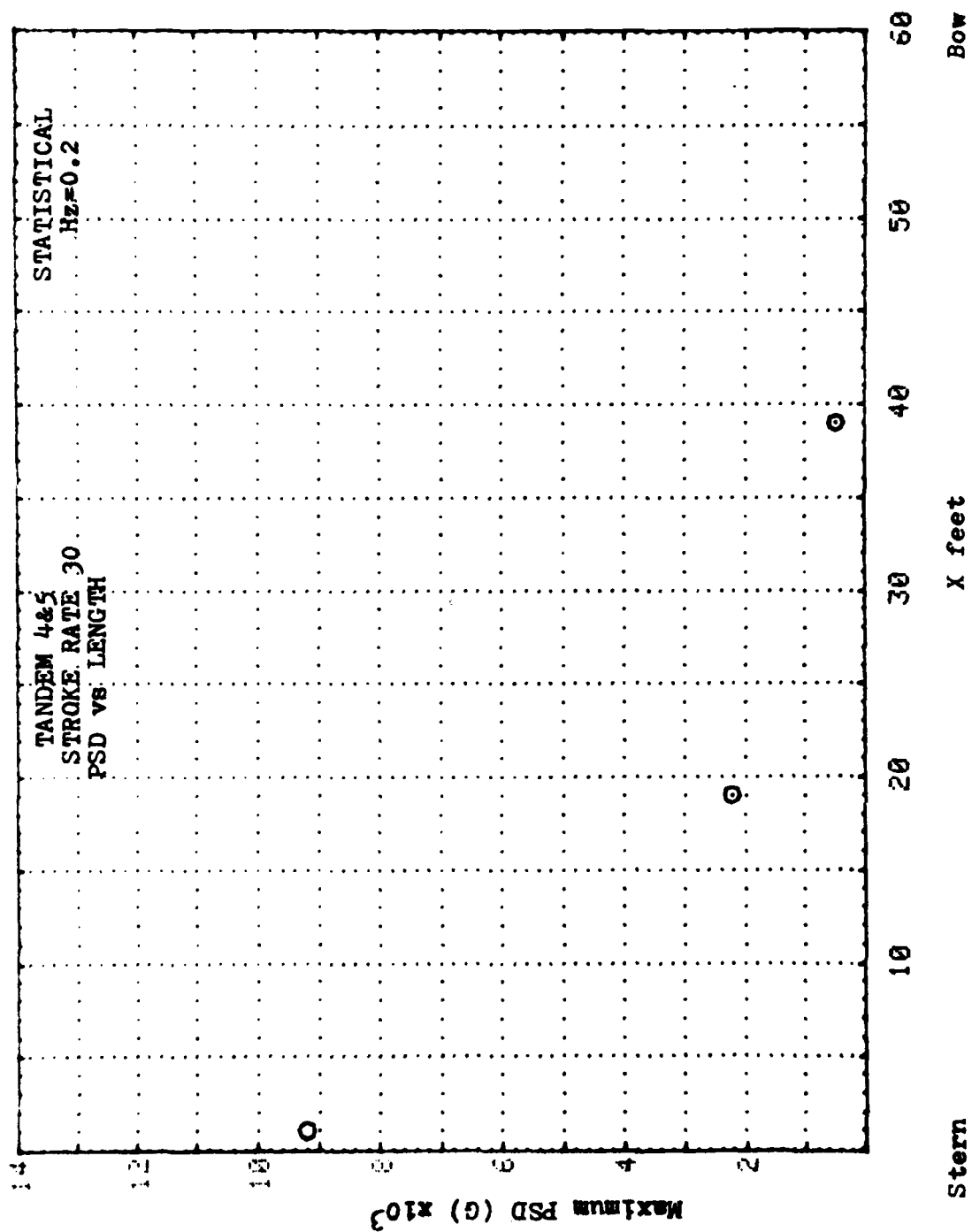


Figure 5

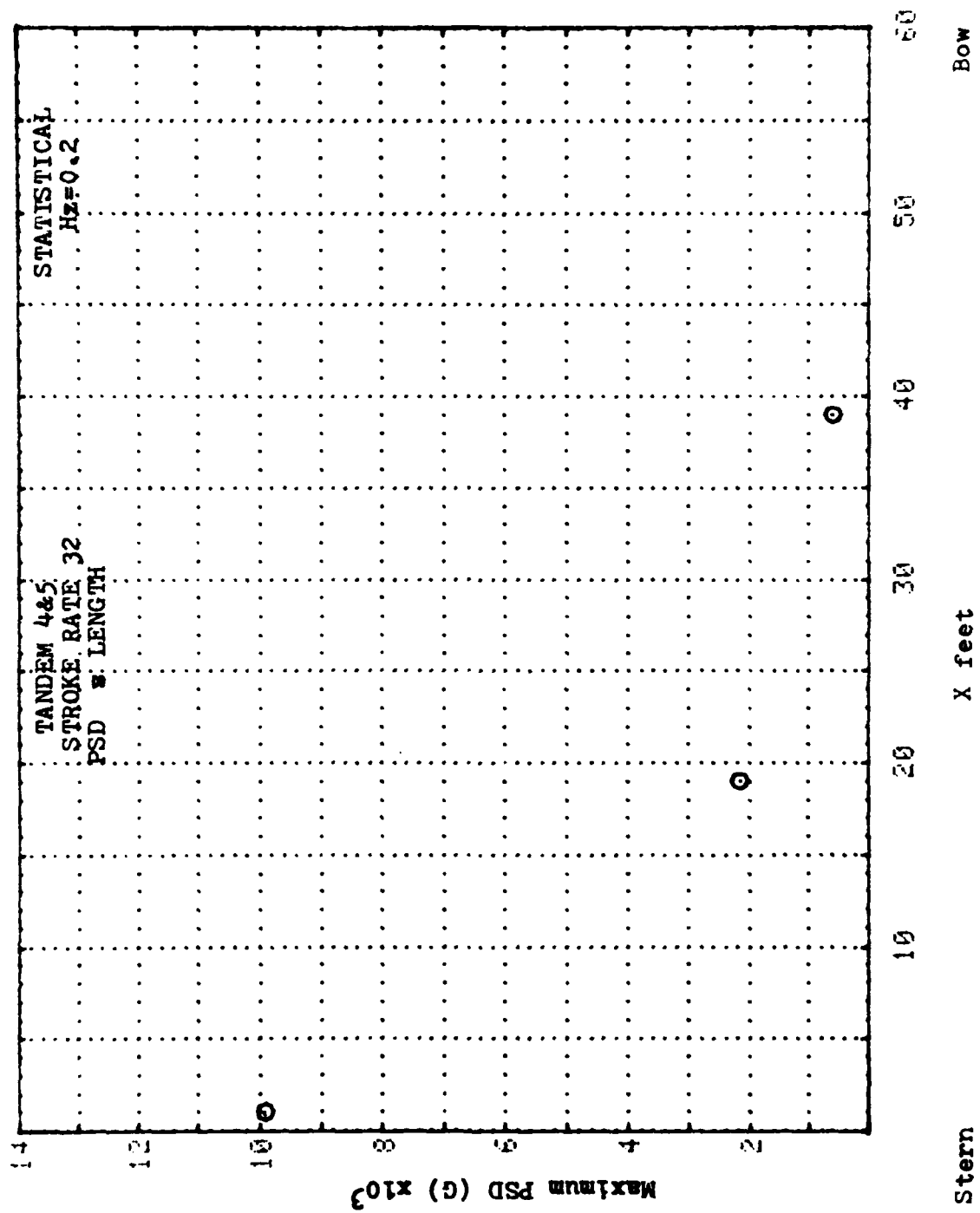


Figure 6

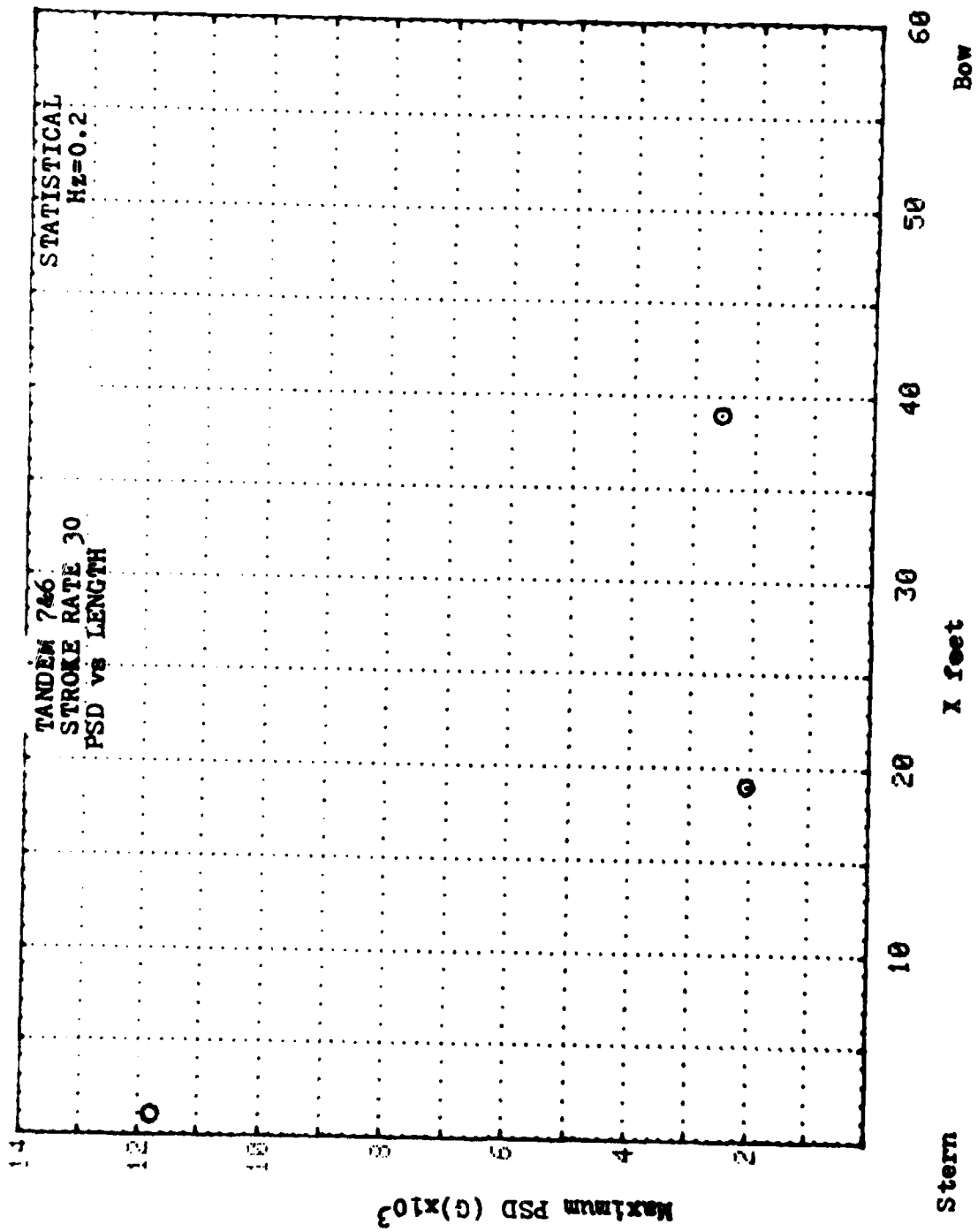


Figure 7

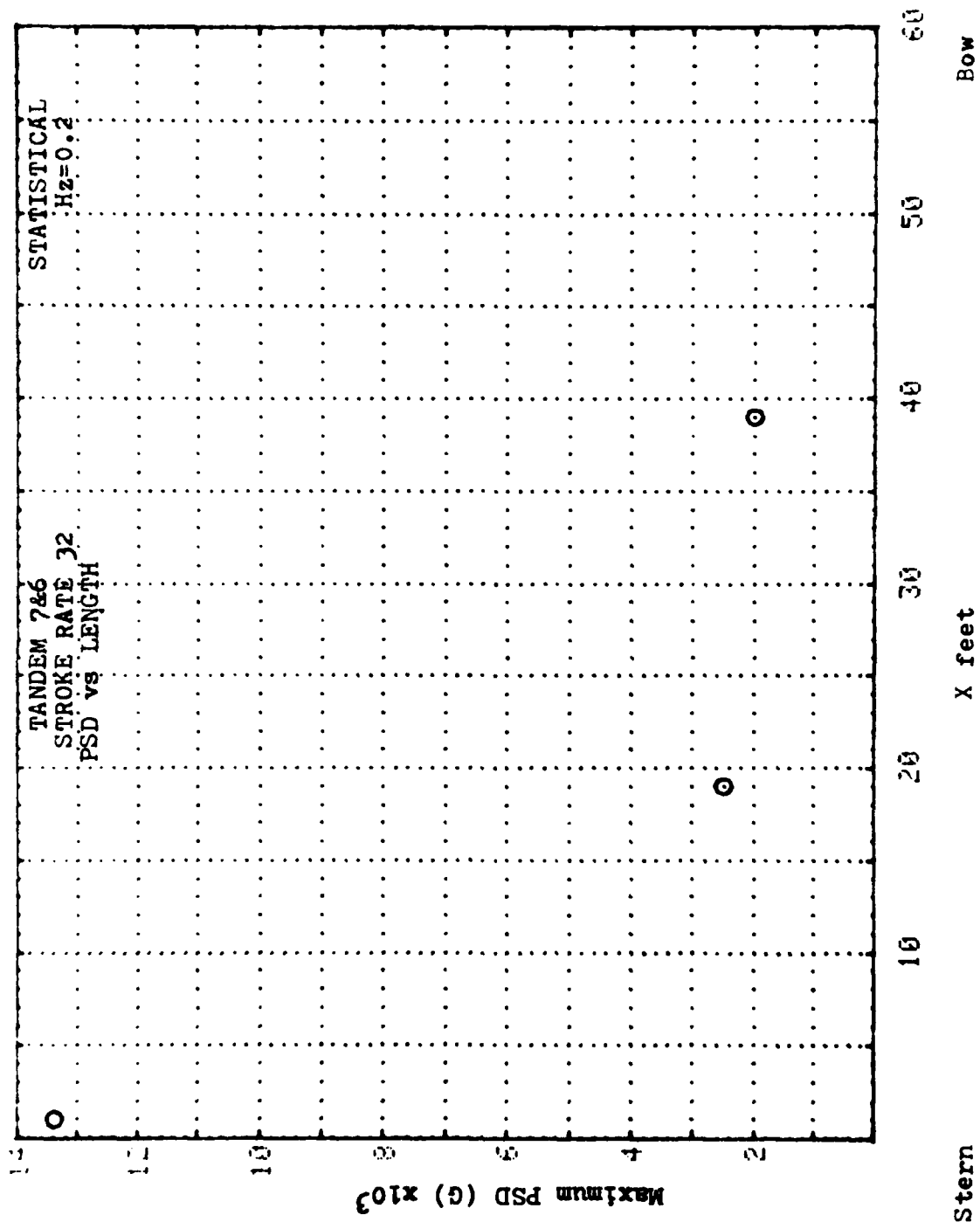


Figure 8

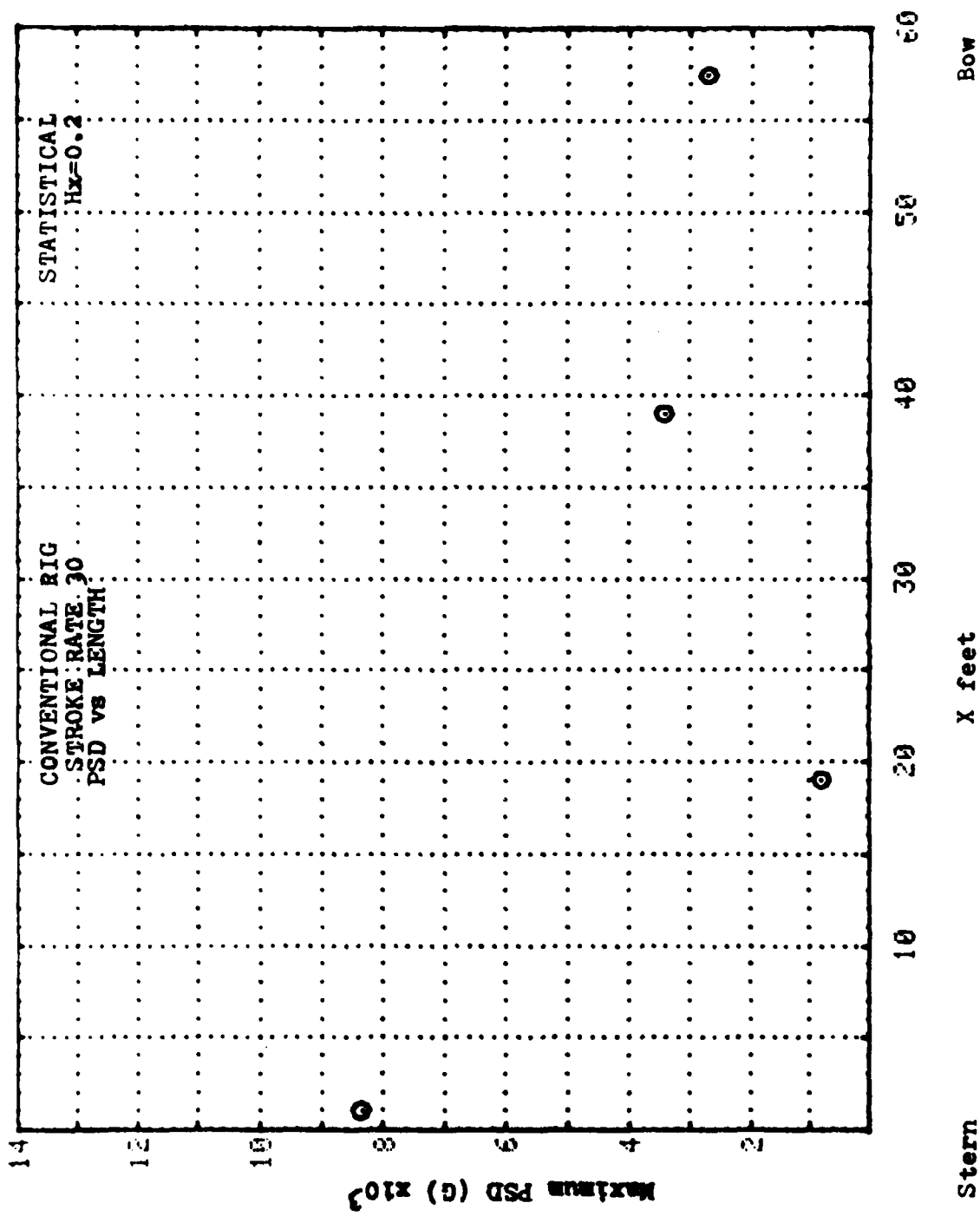


Figure 9

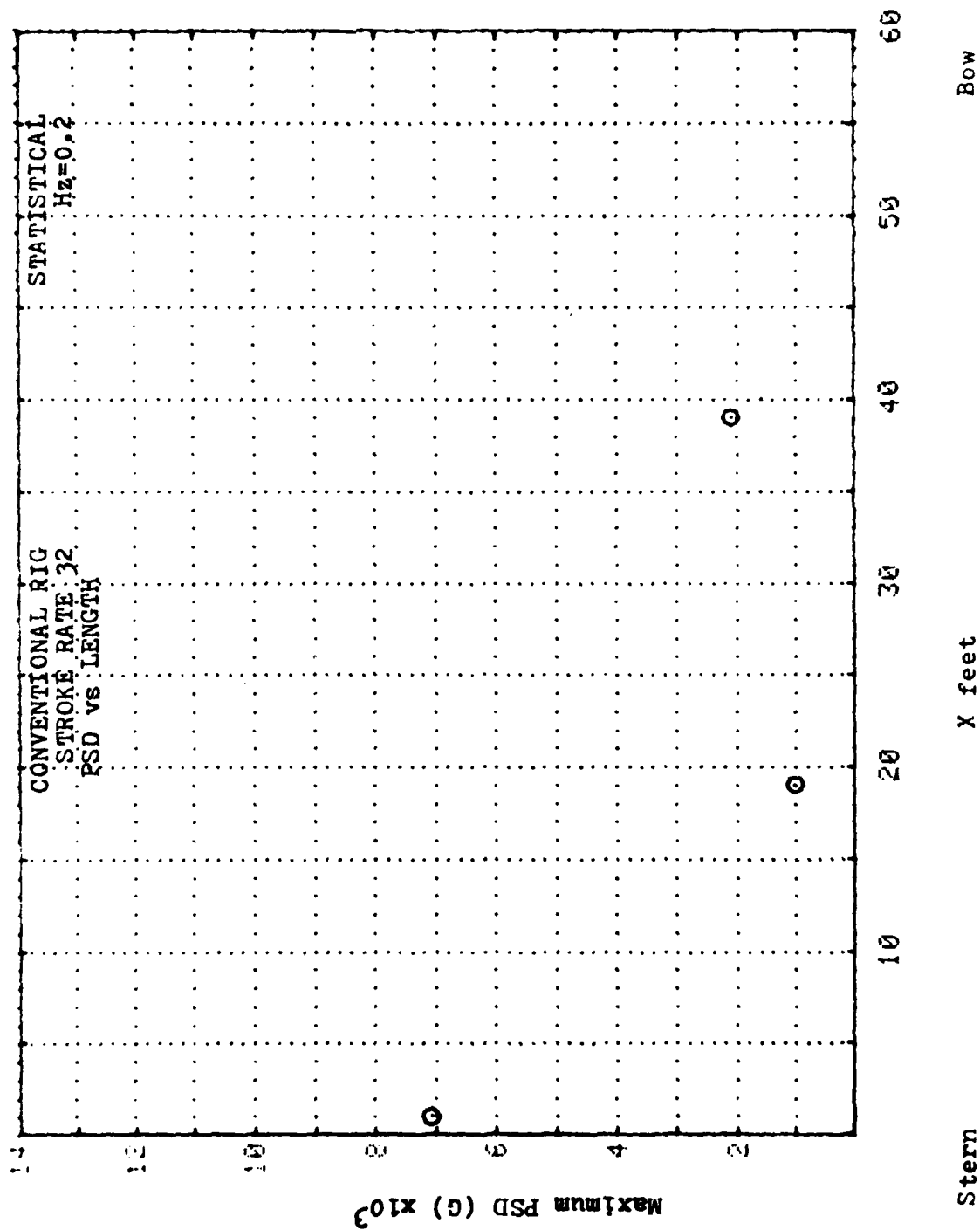


Figure 10

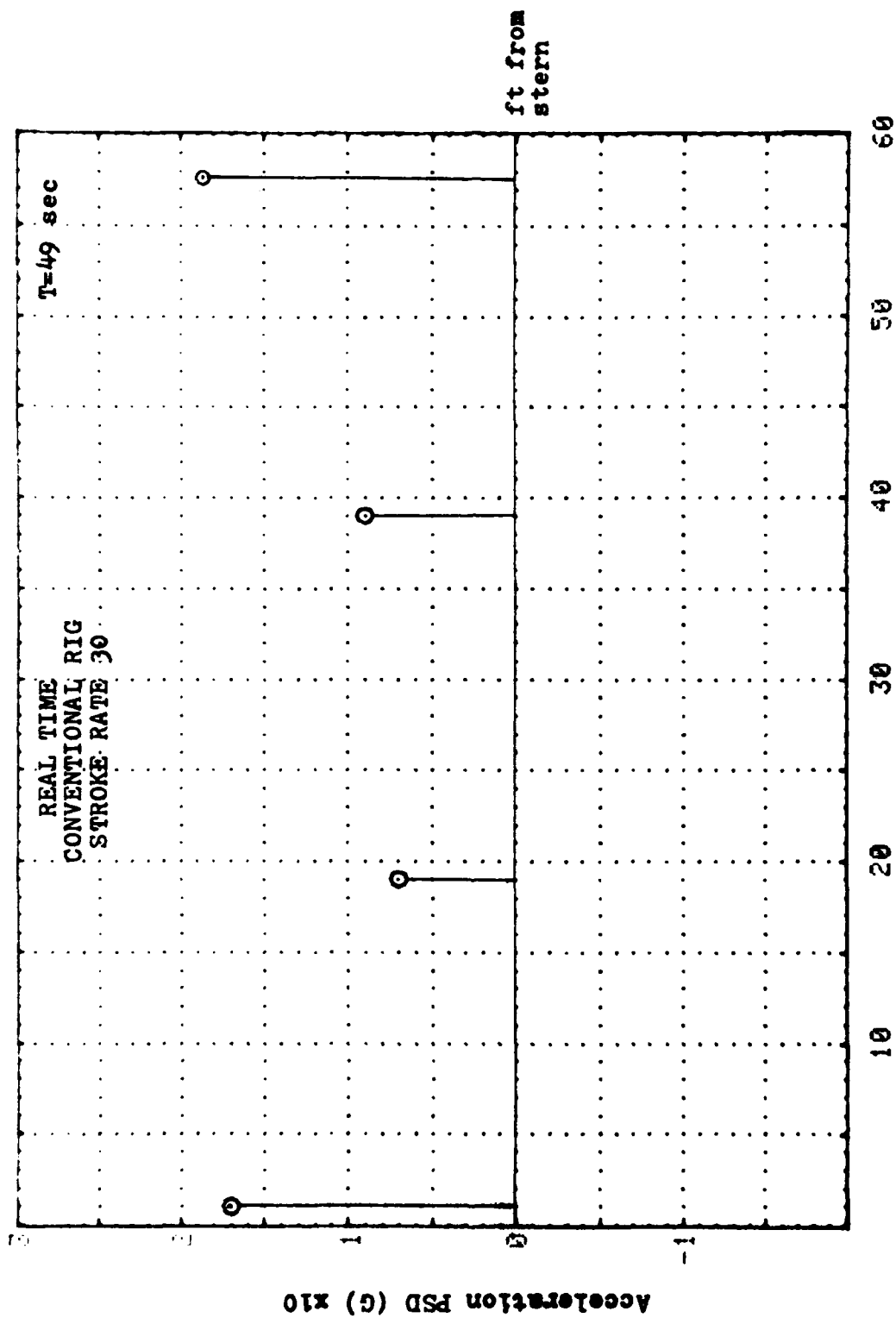


Figure 11

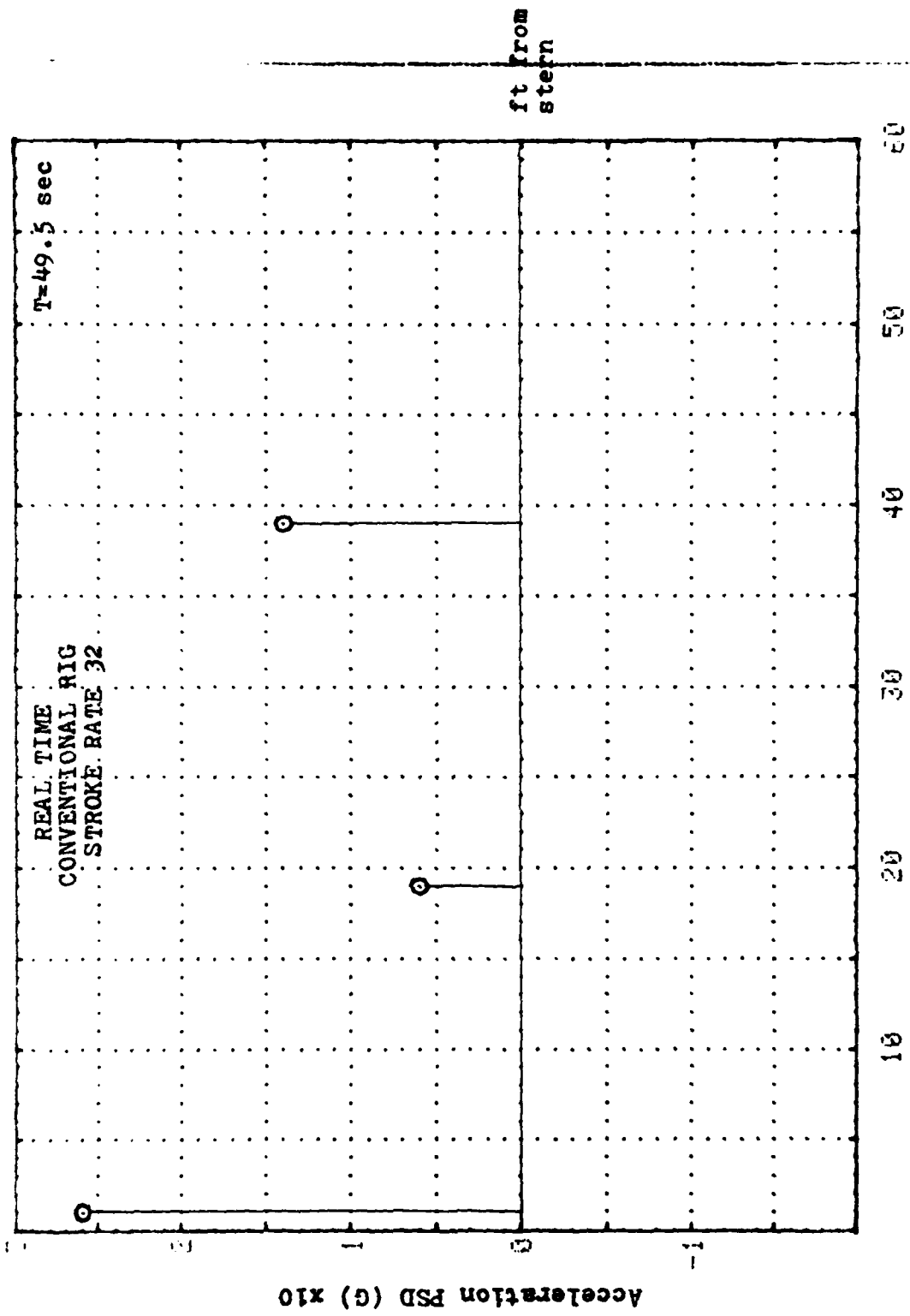
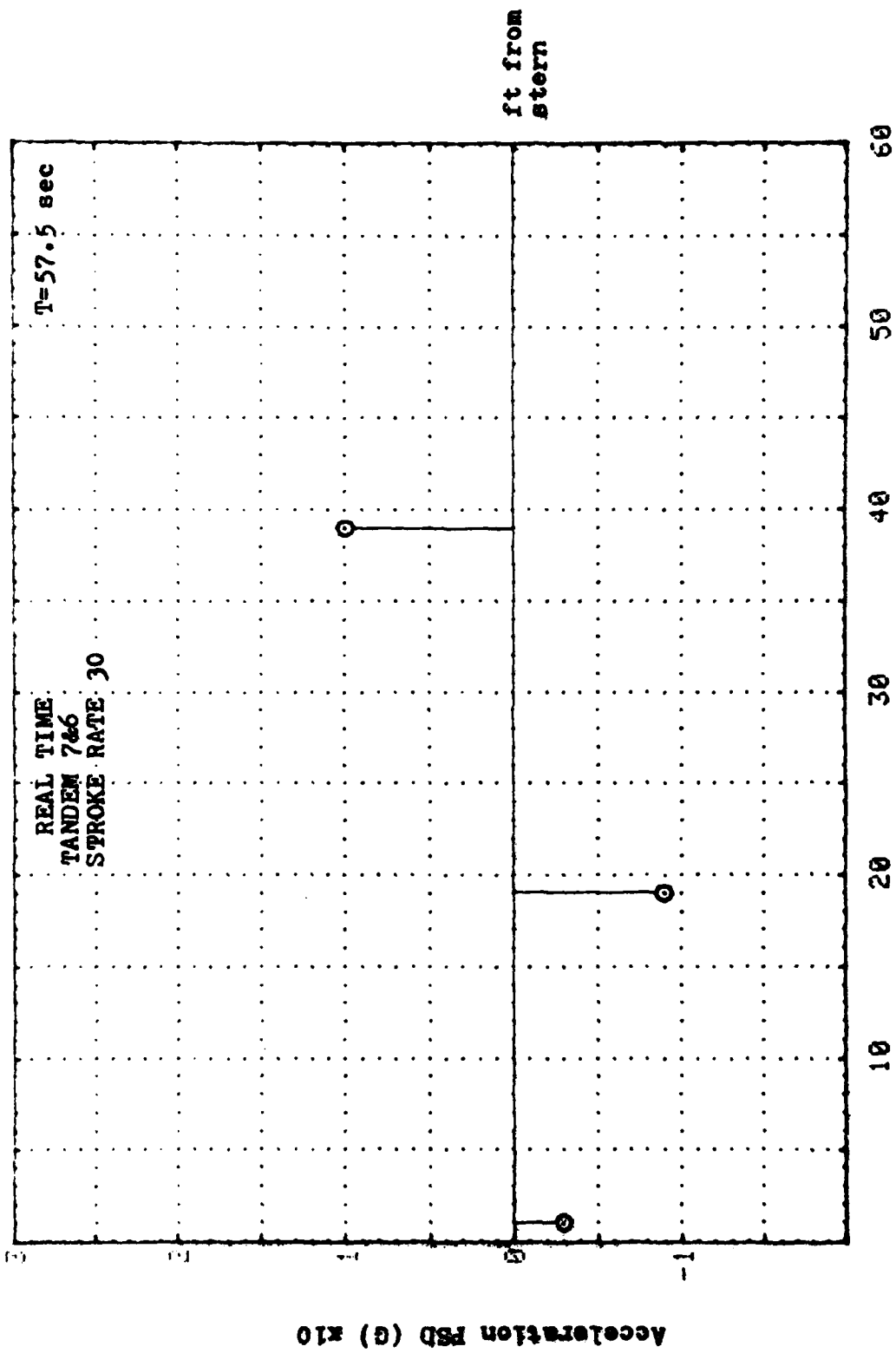


Figure 12



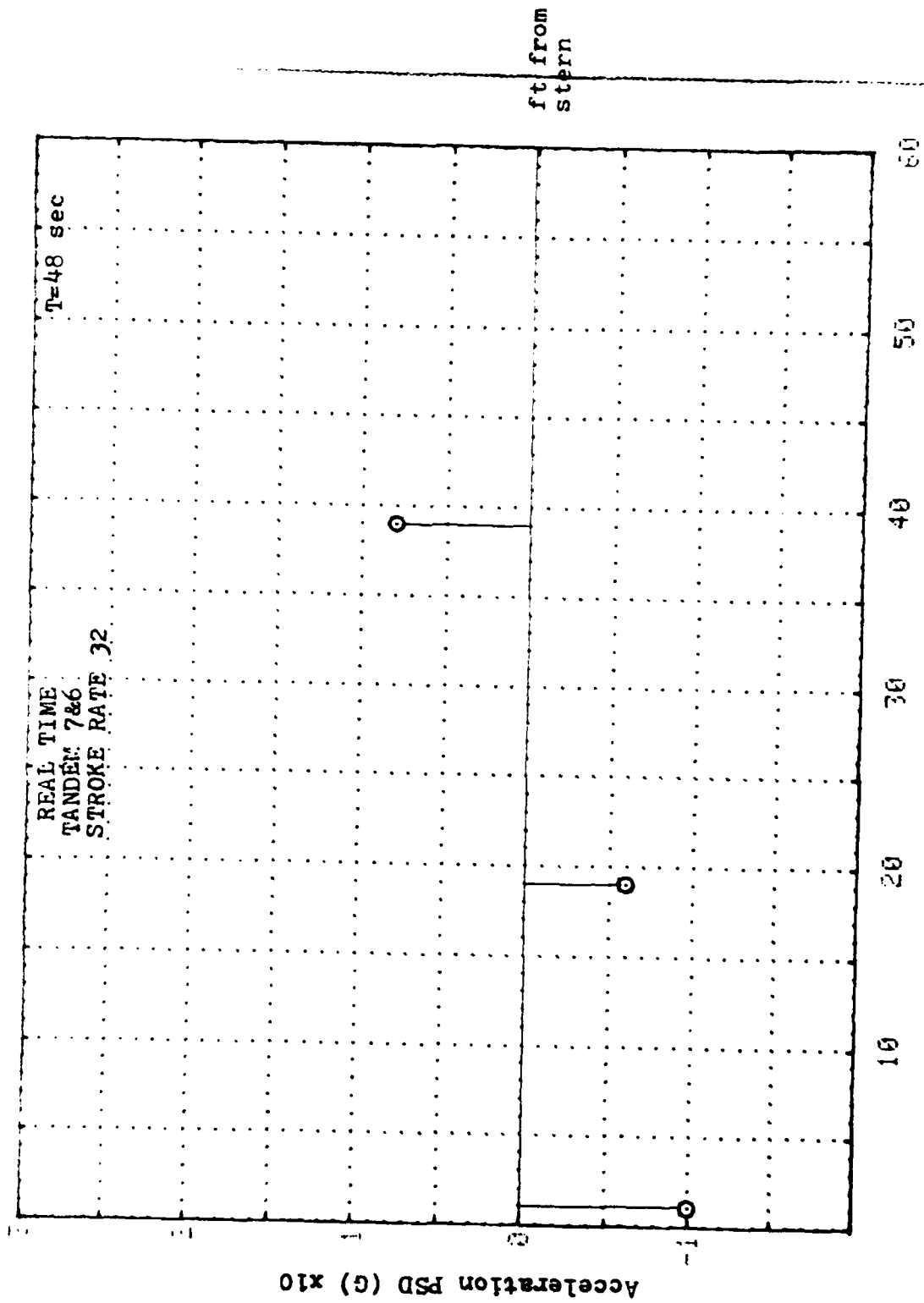
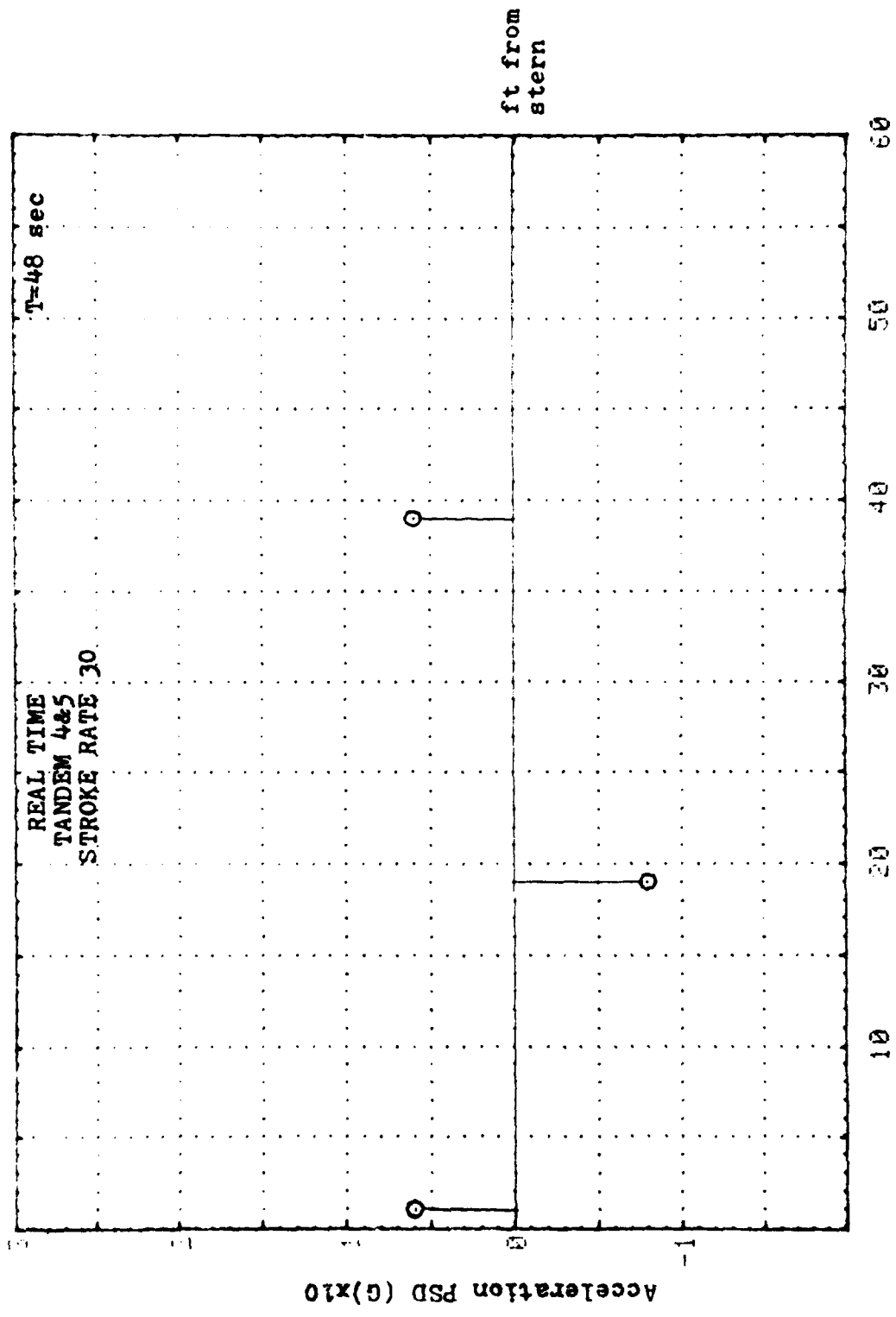


Figure 14



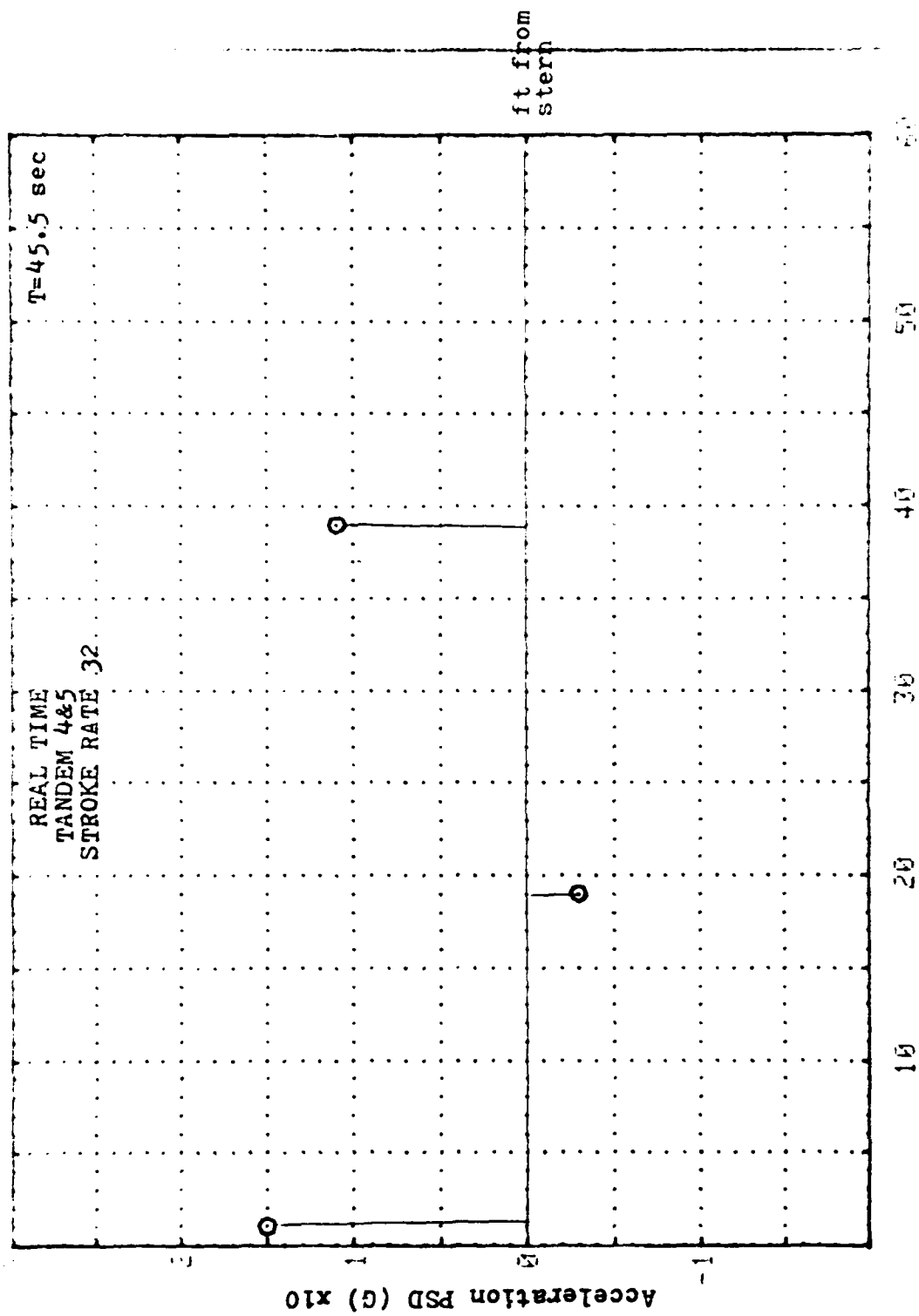


Figure 16

DISCUSSION OF RESULTS

Having to rate which rigging configuration is the best is for the most part still suggestive. However, presented here are some experimental facts obtained from an original full-scale test to help support a coach's view as to which one he uses. Of the three rigging configurations tested, the tandem rigging at seats 7 and 6 provided the best arrangement of side forces. By cancelling one another, similar to a sine wave, this rigging allows the shell to travel in the straightest course reducing the coxswain's frequent requirement to use his rudder.

Tandem at 4 and 5 seats yielded a graph that seems to illustrate that the shell has a definite pivot point located near the 2 seat. With this obvious pivot point, the rudder is presented with a large moment arm, hence reducing the amount of rudder needed to make course changes and/or corrections.

The conventional rig presents a definite side force, hence requiring the coxswain's use of the rudder

to continue in a straight course.

It must be kept in mind that while this report chooses one rigging over another, each crew has its own independent personality, for a team's physical rowing ability and personal chemistries may have a bearing as to which rigging configuration is used. However, this report presents a point from which a coach can start to decide on the rigging configuration that will best suit his crew.

FUTURE WORK

In an effort to continue along this area of experimentation, further work can be done to improve the results from this original trial. Now available from the U.S.N.A. Naval Systems Department is a self-powered recorder. This recorder has the same features as the one used during the test but is smaller and compacted into one unit so that it could be operated from the coxswain's lap. From this point of operation no chase boat would be required, thus alleviating any dampening action on the shell by the trailing wire. Also, this unit has the capability of using 16 transducers vice 4. Therefore more data points could be obtained for a better overall correlation and print out of just what is actually happening. In addition to checking the motion in the transverse axis, data could be collected from points where nodes are expected to occur and measurements made of the longitudinal accelerations.

Acknowledgements

I would like to thank the following people for their help on my research project; it was very much appreciated.

Project Adviser - Prof. Sander Calisal

Electrical Equipment Set-up - Carvel Holton

Computer Analysis - John Hoyt

Members of the Navy's Light Weight Crew Team

REFERENCES

Landweber, L. and M. C. de Macagno, "Added Mass of Two-Dimensional Forms Oscillating in a Free Surface." Journal of Ship Research, November, 1957.

Noonan, E. F. and S. Feldman, "State of the Art for Shipboard Vibration and Noise Control." SNAME Symposium on Ship Vibration, Arlington, Virginia, October 16 - 17, 1978.

SNAME, "Code for Shipboard Vibration Measurements." January, 1976.

SNAME, "Code for Local Shipboard Structures and Machinery Vibration Measurements." December, 1976.

Calisal, S. M. "Ship Hull Vibration," Class Notes.

Appendix A
Equipment Set-up Sketch

EQUIPMENT CHECKLIST

2 - 12V batteries

Abbott DC/AC Inverter

AC junction box

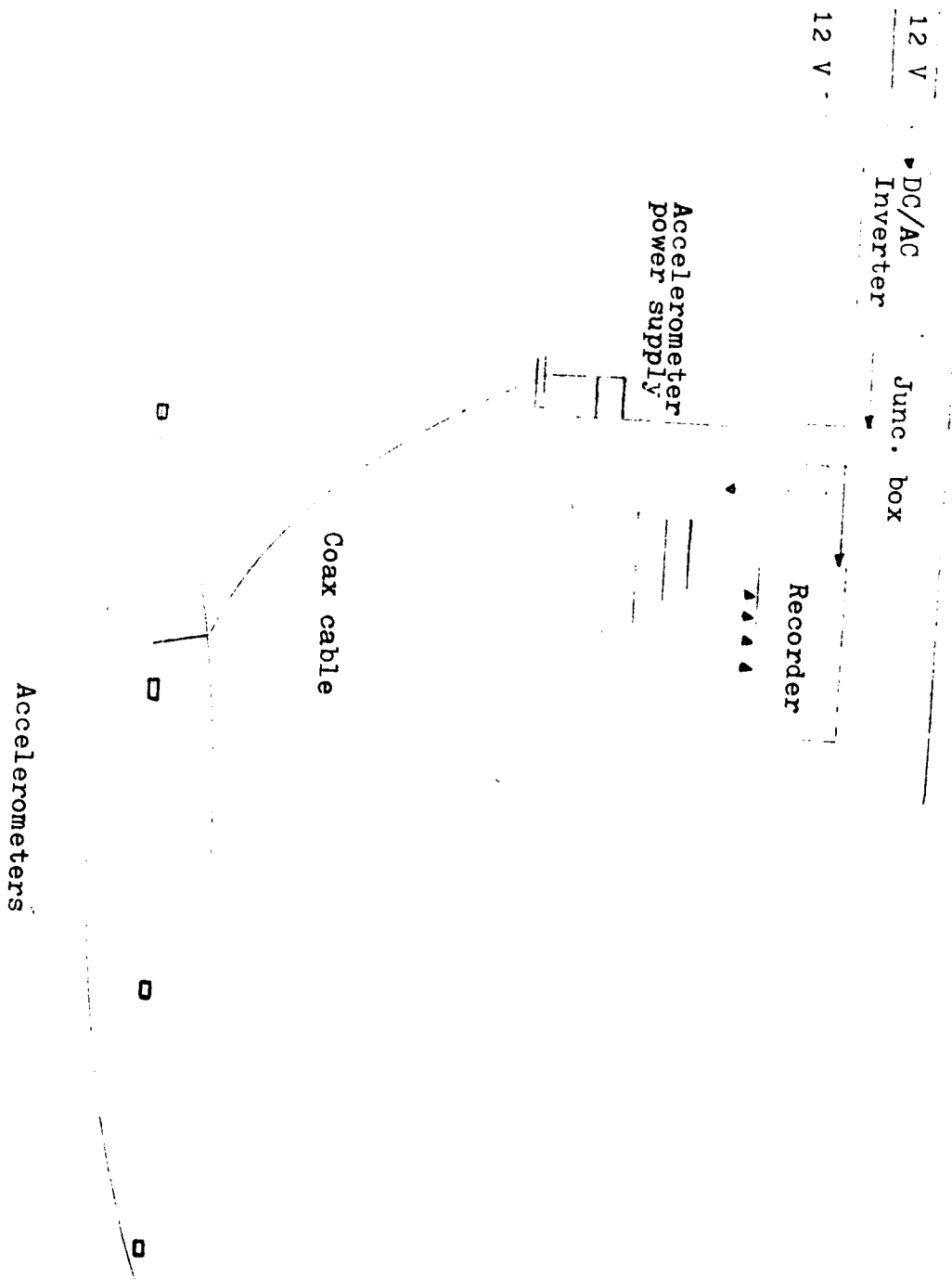
Vetter 4 channel recorder
with microphone and headset

Accelerometer power supply box

Coax cable
with 100 ft shock compliance cord used
between the chase boat and the shell

4 - 1g. accelerometers

Inside the chase boat



Appendix B
Computer Program and Required Data

"Added Mass of Two-Dimensional Forms Oscillating in a Free Surface"
 Dr. L. Landweber and M. C. deMologna, Journal of Ship Research, Nov 1979.

$$C_H = \frac{2 A_H}{\pi \rho H^2}$$

$$G = \frac{S}{2bH} = \frac{S}{2\lambda b^2}$$

$$\lambda = \frac{H}{b}$$

C_H = added mass coefficient corresponding to

A_H = added mass for horizontal vibrations on surface

H = draft of profile (depth)

b = half beam of profile (width)

S = area of profile

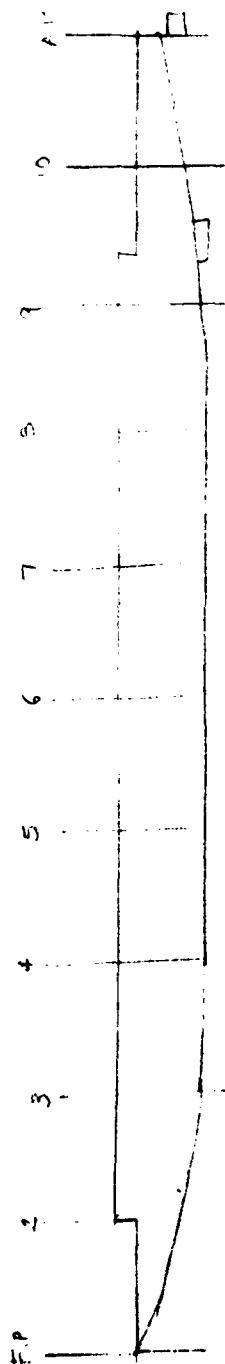
p = fresh water @ 59⁰f
 1.938 16 sec⁴/ft⁴

Sta	b	H	S	λ	G	C_H^*
2	4.56 in	2.38 in	13.44 in	0.52	0.62	0.45
3	7.94	3.44	35.20	0.43	0.64	0.44
4	10.25	4.00	59.12	0.39	0.72	0.42
5	11.63	4.09	68.96	0.35	0.72	0.42
6	10.94	4.19	67.04	0.38	0.73	0.42
7	10.63	4.38	63.52	0.41	0.68	0.43
8	9.56	4.06	55.12	0.42	0.71	0.42
9	7.88	3.81	44.32	0.48	0.74	0.41
10	4.50	3.38	17.84	0.75	0.59	0.47

* from Fig. 5

$$\text{Added Mass } A_H = \frac{C_H \pi \rho H^2}{2}$$

Sta	A_H
2	0.053 16 sec ² /ft ²
3	0.110
4	0.142
5	0.148
6	0.155
7	0.174
8	0.146
9	0.125
10	0.113



Sta	2	3	4	5	6	7	8	9	10
EI	1.73×10^9	3.38×10^9	4.88×10^9	5.02×10^9	5.26×10^9	4.87×10^9	4.25×10^9	3.80×10^9	1.75×10^9
X	70.2	140.4	2.0.6	380.8	351.0	421.2	491.4	561.6	631.8
Z	10^{-10}	10^{-10}	10^{-10}	10^{-10}	10^{-10}	10^{-10}	10^{-10}	10^{-10}	10^{-10}
KAG	10^{10}	10^{10}	10^{10}	10^{10}	10^{10}	10^{10}	10^{10}	10^{10}	10^{10}
M_I	26.72	220.66	220.69	220.69	220.70	220.72	220.69	220.67	26.78
M_T	26.72	230.94	230.97	230.97	230.98	231.00	230.97	230.95	26.78
I	132.9	260.26	375.7	386.19	404.51	394.27	327.07	292.27	134.82

Key x; Distance to bow in inches

M_I ; Mass per unit length at station

M_T ; Mass per unit length at station including oars

Z; Rotary inertia large No. used for not

KAG; Shear deformation interest in their effect

E; 13×10^8 psi

Appendix C

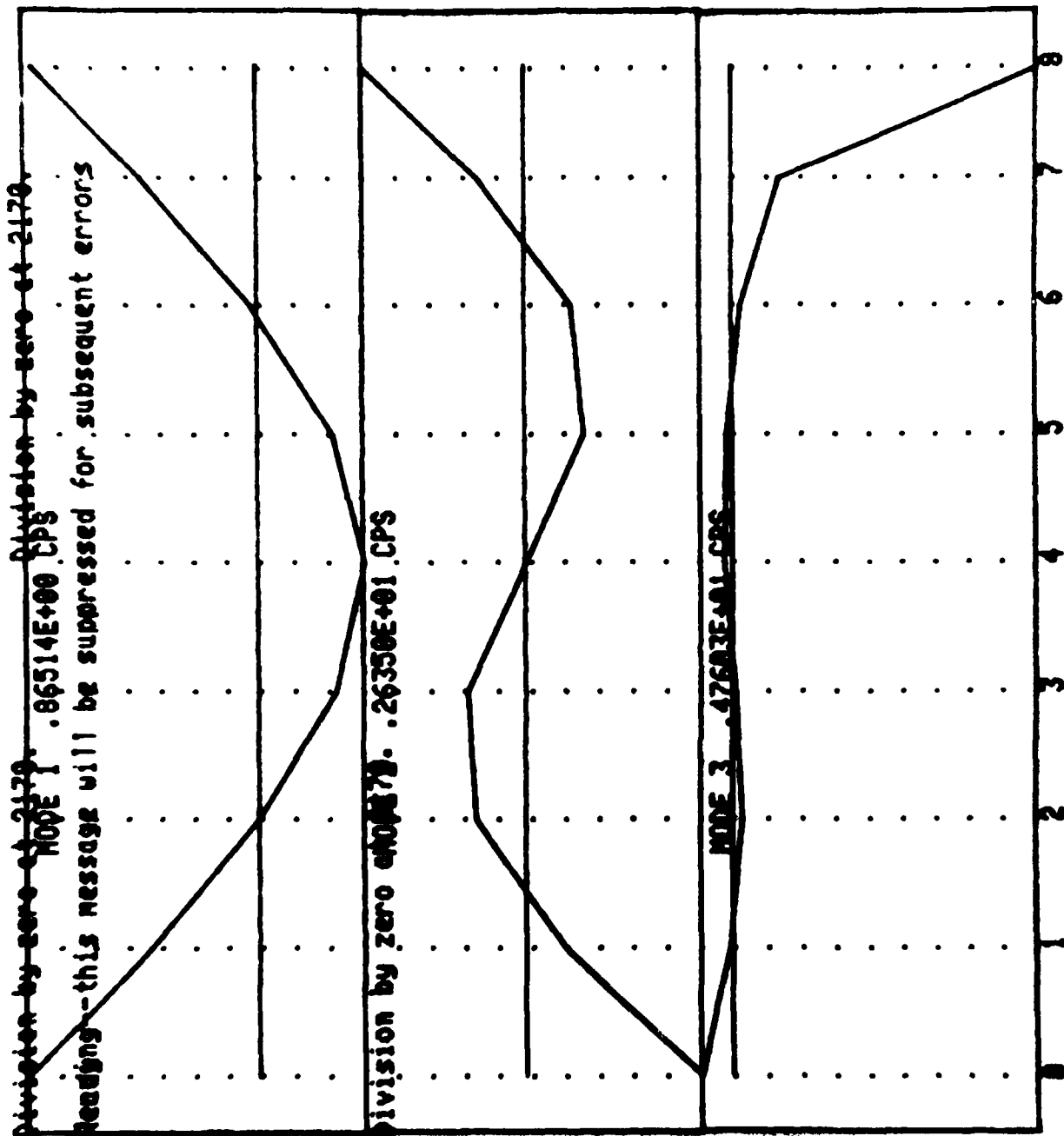
Natural Vibration Modes Computer Output

Division by zero at 2170. Division by zero at 2170.
NODE 1. .06136E+00 CPS
Reading--this message will be suppressed for subsequent errors

Division by zero at 2171. .26148E+01 CPS

Division by zero at 2172. 4.92235E+01 CPS

With Oars



Appendix D

Test Data

Test Data

Oarsmen

Bow	Jim Yohe
2	Mike Hamele
3	Chuck Smith
4	Charlie Kanewske
5	Dave Wessing
6	Rob Niewoehner
7	Fred Tettetbach
Stroke	Jim Genter
Cox	Dan Pederson

Location of Accelerometers

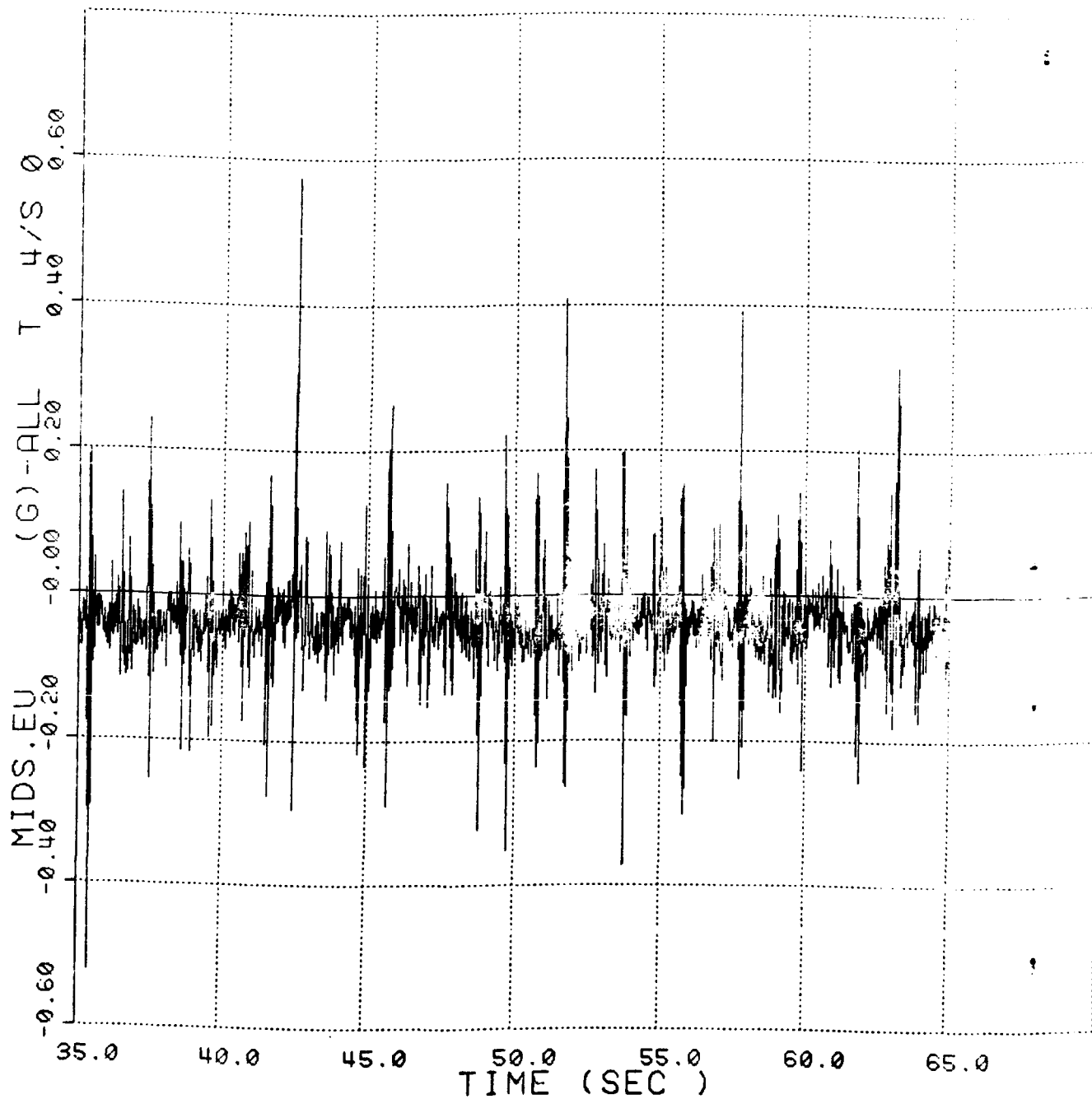
STERN	.	.	.	BOW
1 ft.
		19 ft.		
			39 ft.	
				1 ft. (57.5)

Course- College Creek @ 500 meters

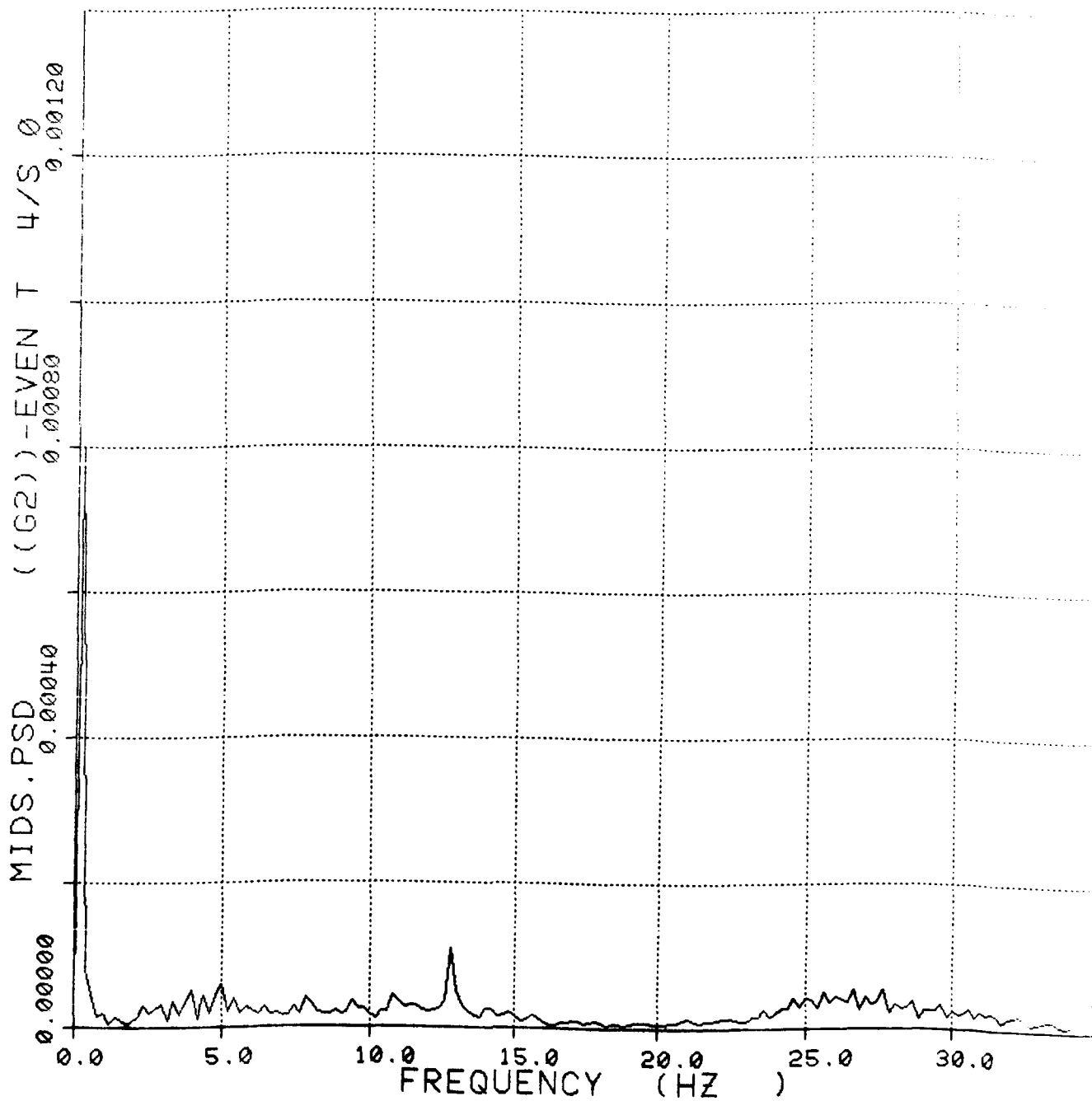
Conditions- Raining lightly
Calm Water
No wind

Appendix E
Computer Printout

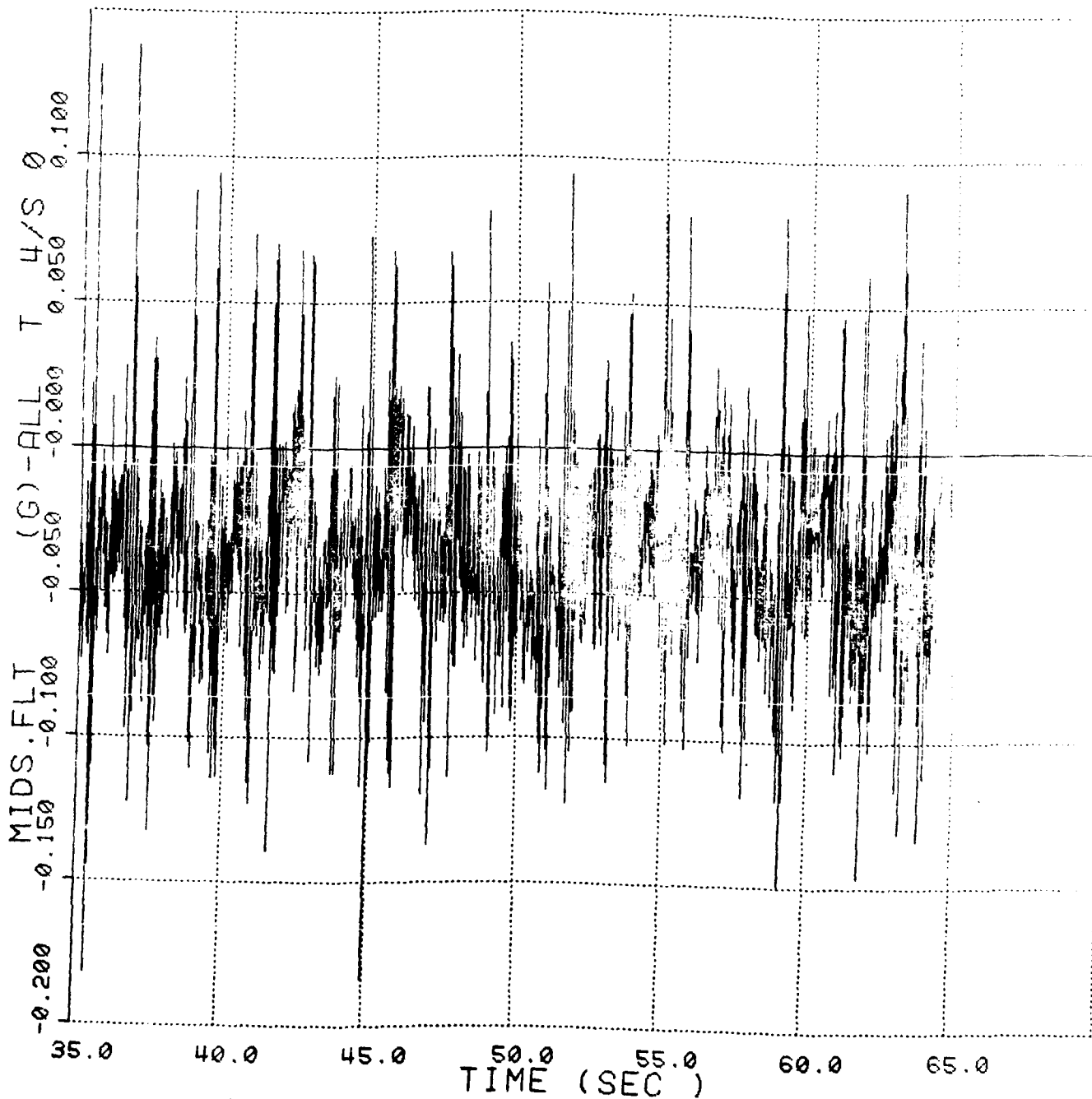
TEST: 4 RUN NO: 1 DATE:07-APR-80 TIME:10:50:47



TEST: 4 RUN NO: 1 DATE:07-APR-80 TIME:10:52:49

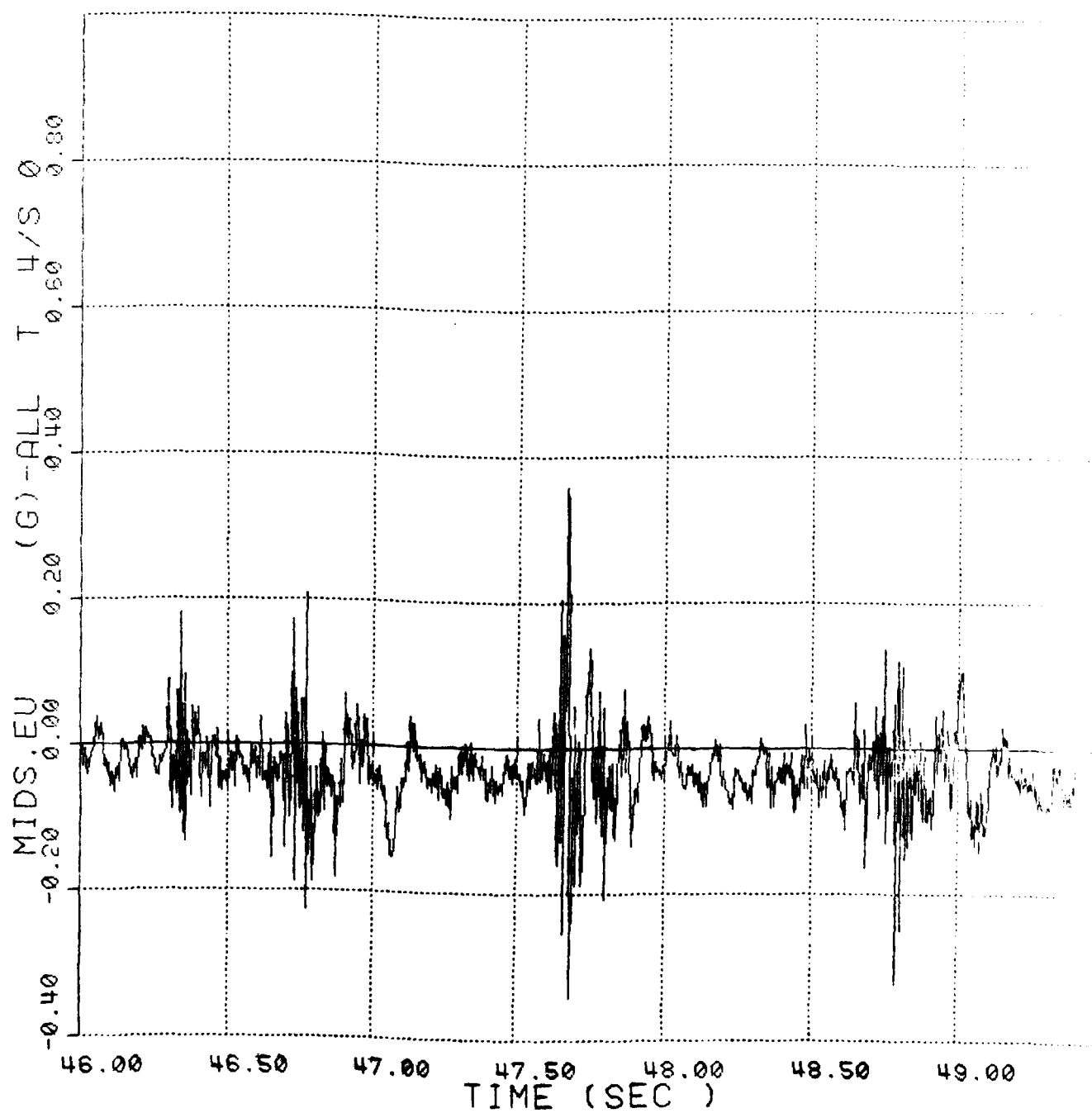


TEST: 4 RUN NO: 1 DATE: 07-APR-80 TIME: 10:56:39

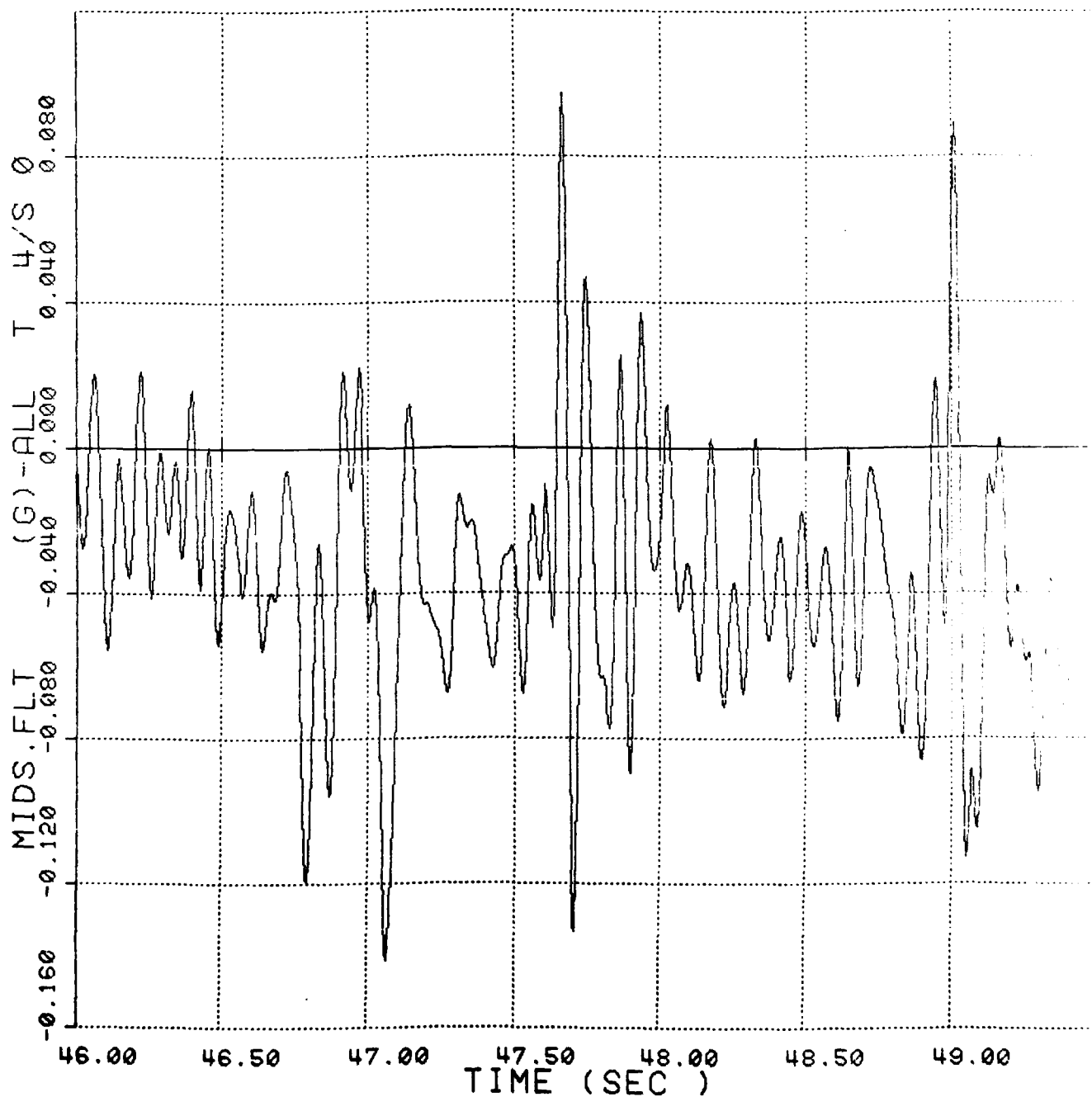


E-3-Blank

TEST: 4 RUN NO: 1 DATE: 07-APR-80 TIME: 10:58:53



TEST: 4 RUN NO: 1 DATE:07-APR-80 TIME:11:00:36



DATE
FILMED
-8